A Mathematical Model of Cardiocyte Ca^{2+} Dynamics with a Novel Representation of Sarcoplasmic Reticular Ca^{2+} Control

Steven M. Snyder, Bradley M. Palmer, and Russell L. Moore
Department of Kinesiology and Applied Physiology, The University of Colorado Cardiovascular Institute (CUCVI), University of Colorado, Boulder, Colorado 80309-0354 USA

ABSTRACT Cardiac contraction and relaxation dynamics result from a set of simultaneously interacting Ca^{2+} regulatory mechanisms. In this study, cardiocyte Ca^{2+} dynamics were modeled using a set of six differential equations that were based on theories, equations, and parameters described in previous studies. Among the unique features of the model was the inclusion of bidirectional modulatory interplay between the sarcoplasmic reticular Ca^{2+} release channel (SRRC) and calsequestrin (CSQ) in the SR lumen, where CSQ acted as a dynamic rather than simple Ca^{2+} buffer, and acted as a Ca^{2+} sensor in the SR lumen as well. The inclusion of this control mechanism was central in overcoming a number of assumptions that would otherwise have to be made about SRRC kinetics, SR Ca^{2+} release rates, and SR Ca^{2+} release termination when the SR lumen is assumed to act as a simple, buffered Ca^{2+} sink. The model was sufficient to reproduce a graded Ca^{2+}-induced Ca^{2+} release (CICR) response, CICR with high gain, and a system with reasonable stability. As constructed, the model successfully replicated the results of several previously published experiments that dealt with the Ca^{2+} dependence of the SRRC (Fabiato, 1985, *J. Gen. Physiol.* 85:247–289), the refractoriness of the SRRC (Cheng et al., 1996, *Am. J. Physiol.* 270:C148–C159), the SR Ca^{2+} load dependence of SR Ca^{2+} release (Bassani et al., 1995, *Am. J. Physiol.* 268:C1313–C1329; Gilchrist et al., 1992, *J. Biol. Chem.* 267:20850–20856), SR Ca^{2+} leak (Wier et al., 1994, *J. Physiol. (Lond.).* 474:463–471; Bassani and Bers, 1995, *Biophys. J.* 68:2015–2022), SR Ca^{2+} load regulation by leak and uptake (Ginsburg et al., 1998, *J. Gen. Physiol.* 111:491–504), the effect of Ca^{2+} trigger duration on SR Ca^{2+} release (Bers et al., 1990, *Am. J. Physiol.* 258:C944–C954), the apparent relationship that exists between sarcoplasmic and sarcoplasmic reticular calcium concentrations (Shannon and Bers, 1997, *Biophys. J.* 73:1524–1531), and a variety of contraction frequency-dependent alterations in sarcoplasmic $[Ca^{2+}]$ dynamics that are normally observed in the laboratory, including rest potentiation, a negative frequency-$[Ca^{2+}]$ relationship, and extrasystolic potentiation. Furthermore, under the condition of a simulated Ca^{2+} overload, an alternans-like state was produced. In summary, the current model of cardiocyte Ca^{2+} dynamics provides an integrated theoretical framework of fundamental cellular Ca^{2+} regulatory processes that is sufficient to predict a broad array of observable experimental outcomes.

INTRODUCTION

The regulation of cytosolic Ca^{2+} concentration, $[Ca^{2+}]_c$, in cardiac myocytes has been recognized to be the predominant determinant of cardiac contraction and relaxation dynamics (Bers, 1993). The experimental identification and characterization of the many $[Ca^{2+}]_c$ regulatory mechanisms in cardiac myocytes have been paramount in classifying the relative importance of the calcium-dependent factors that influence cardiac function. Developing and testing hypotheses regarding the complex and interdependent relationships of these $[Ca^{2+}]_c$ regulatory mechanisms has been the principal focus of mathematical modeling in this field. Various models have been developed to describe $[Ca^{2+}]_c$ regulation in cardiac myocytes (Bers and Berlin, 1995; Earm and Noble, 1989; Hilgemann and Noble, 1987; Harrison et al., 1992; Langer and Peskoff, 1996; Peskoff et al., 1992; Smith et al., 1998; Tang and Othmer, 1994; Stern, 1992; Wong et al., 1992). Of particular importance have been those models that have attempted to thoroughly describe the temporal qualities of $[Ca^{2+}]_c$ based on characteristics of Ca^{2+} accumulation and release from intracellular compartments and buffers. These types of models have evolved to the point where they are sufficient to make reasonable predictions of intracellular $[Ca^{2+}]$ dynamics under very simple simulated experimental conditions. Collectively, these types of theoretical models have provided invaluable insights into the concerted mechanisms that regulate intracellular Ca^{2+} dynamics in the heart. In general, however, virtually none of these models have been shown to be sufficient to accommodate predictions of intracellular Ca^{2+} dynamics under multiple and more complex experimental conditions. More recently, much of the modeling in this area has attempted to describe hypothetical cellular mechanisms that sufficiently represent fundamental properties of excitation-contraction coupling (Stern, 1992; Rice et al., 1999; Jafri et al., 1998), which would include a Ca^{2+}-induced Ca^{2+} release (CICR) mechanism that demonstrates graded responsiveness to a sarcolemmal Ca^{2+} trigger, high gain, and reasonable stability.

In this study, we propose a novel model of sarcoreticular Ca^{2+} regulation where control of CICR exhibits the fundamental characteristics of graded sarcoplasmic reticulum

Received for publication 3 February 1999 and in final form 20 March 2000.

Address reprint requests to Dr. Russell L. Moore, Campus Box 354, Department of Kinesiology and Applied Physiology, University of Colorado, Boulder, CO 80309-0354. Tel.: 303-492-5209; Fax: 303-492-4009; E-mail: rmoore@spot.colorado.edu.

0006-3495/00/07/94/22 $2.00

(SR) Ca^{2+} release, high gain, and stability and is dependent upon the regulation of SR Ca^{2+} release channels (SRRCs) by $[Ca^{2+}]$ changes in a confined subspace ("fuzzy space"; Lederer et al., 1990) and by Ca^{2+} sensing elements in the SR lumen. Overall, the purpose of this study was to develop a macroscopic model of cardiocyte sarcoreticular Ca^{2+} regulation that 1) is based on previously described control theories and parameter values; 2) possesses a quiescent steady-state (starting point) condition that was self-defined by the same model control elements that governed dynamic model responses; 3) is sufficient to predict expected outcomes from multiple and relatively complex experimental perturbations; 4) is designed to provide predictions of experimentally observable whole-cell $[Ca^{2+}]_c$ responses; and 5) could be used as a framework around which more "microscopic" theories of Ca^{2+} regulation could be included.

As constructed, the model was sufficient to replicate the results of several simple but very different types of experiments that appear in the literature (Bassani and Bers, 1995; Bassani et al., 1995; Bers et al., 1990; Cheng et al., 1996; Fabiato, 1985; Gilchrist et al., 1992; Ginsburg et al., 1998; Shannon and Bers, 1997; Wier et al., 1994), as well as predictions of the sarcoplasmic $[Ca^{2+}]$ transient that would be expected to occur in response to alterations in myocyte pacing frequency, the delivery of extrasystolic intervals at a variety of background pacing frequencies, and cellular Ca^{2+} overload (alternans). Critical examination of the results of the current study should provide insights into theoretical mechanisms of control of sarcoreticular Ca^{2+} cycling in the heart.

MATERIALS AND METHODS

Model overview

A simple schematic of the key elements of cardiocyte Ca^{2+} control represented in our model is depicted in Fig. 1. Briefly, our model was constructed to account for Ca^{2+} movement between an extracellular compartment and a very small, restricted, or fuzzy space (Lederer et al., 1990) that exists between the t-tubular membrane and the terminal cisternal face of the sarcoplasmic reticulum. Calcium buffering specific to the "fuzzy space" is also included. CICR from the SR is mediated by Ca^{2+} movement in the fuzzy space and the interaction of this Ca^{2+} with specific binding sites on the SRRCs. In this regard, it is relevant to note that CICR control characteristics at the level of a single fuzzy space were modeled and then subjected to composite averaging to yield a simulation of whole-cell Ca^{2+} dynamics. One of the novel features of our model is that it contains regulatory interactions that exist between SRRCs, SR luminal $[Ca^{2+}]$, and the predominant luminal SR buffer calsequestrin (CSQ). These types of interactions are implied by considerable experimental evidence (discussed below and in Appendix B) and were included to account for the known effects of SR Ca^{2+} load on SR Ca^{2+} release (Bassani et al., 1995; Donoso et al., 1995; Ikemoto et al., 1989, 1991; Kawasaki and Kasai, 1994; Janczewski et al., 1995; Lukyanenko et al., 1996; Ohkura et al., 1995; Sham et al., 1995; Shannon and Bers, 1997; Zhang et al., 1997). The model includes a diffusional link between Ca^{2+} in the fuzzy space and the cytosol. The cytosolic compartment contains endogenous Ca^{2+} buffers and could accommodate exogenous Ca^{2+} buffering by the Ca^{2+} indicators (fura-2, fluo-3, etc). The exogenous buffer was included to produce model predictions of the types of cytosolic $[Ca^{2+}]$ characteristics that would be observed experimentally and to render the model more amenable to laboratory test.

Regulation of SRRCs by Ca^{2+} in the fuzzy space

In our model, each contraction cycle was initiated by a brief influx of Ca^{2+} into the fuzzy space per the principles previously described (Tang and Othmer, 1994; Langer and Peskoff, 1996). This general method of initiating the model is described in Appendix A and is critically evaluated in the Discussion. Regulation of CICR through SRRCs was assumed to be dependent upon the occupancy of "fast" and "slow" Ca^{2+} binding sites on the SRRCs (Fabiato, 1985; Coronado et al., 1994), and a high degree of binding cooperativity between multiple fast sites was assumed (Fabiato, 1985; Sham et al., 1995). At the single SRRC level, four functional states were assumed and are described in Table 1.

The movement of Ca^{2+} through SRRCs into the fuzzy space was described as a function of the fraction of SRRCs in the open state and the free $[Ca^{2+}]$ gradient between the SR lumen and the fuzzy space. This model provided for a system of control in which SR Ca^{2+} release was 1) initiated by the early influx of Ca^{2+} into the fuzzy space and 2) regeneratively amplified by subsequent elevations in fuzzy space $[Ca^{2+}]$ that

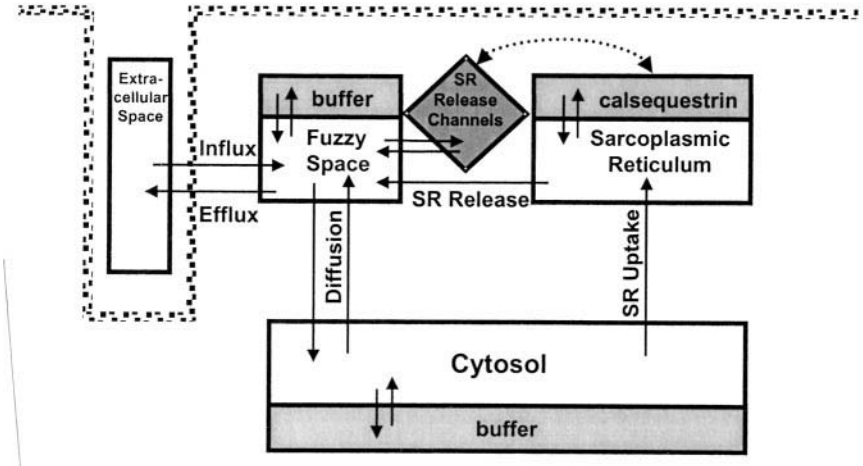

FIGURE 1 Cell schematic for the model, representing three intracellular compartments with buffering, the extracellular space, and the related Ca^{2+} movement processes. The movement of Ca^{2+} through the SR Ca^{2+} release channels (SRRCs) was modeled to be dependent on the Ca^{2+} bound state of the SRRC (see Appendix A and Table 1). Binding states of the SRRC and calsequestrin (CSQ) were designed to be associated by a bidirectional feedback mechanism (Appendix B).

TABLE 1 Four functional SRRC states

SRRC states	"Fast" site	"Slow" site
Activatable	—	—
Open	Ca^{2+}	—
Closed	Ca^{2+}	Ca^{2+}
Refractory	—	Ca^{2+}

occurred as a result of SR Ca^{2+} release into that space. Calcium buffering in each compartment (fuzzy space and the SR lumen) was included and will be discussed in greater detail in the sections that follow. Specific mathematical descriptions of these processes appear in Appendix A.

Interactions between the SRRC and the SR lumen

A unique and functionally important feature of the current model is the inclusion of interactions between the SRRC and the Ca^{2+} load of the SR lumen. In our model, bidirectional interactions between the SRRC and Ca^{2+} in the SR lumen are assumed to be mediated via CSQ. The rationale for proposing this type of interaction derives from a considerable body of experimental evidence from studies on striated muscle preparations. First, in both cardiac and skeletal muscle, CSQ is known to be localized in the terminal cisternal portion of the SR and appears to be attached to the junctional face membrane in close proximity to the SRRCs (Zhang et al., 1997; Brandt et al., 1990). Furthermore, there is now strong evidence that cardiac CSQ and the SRRCs are coupled by junctin and triadin (Zhang et al., 1997). This type of association is consistent with the idea that CSQ and SRRCs are functionally linked. Second, the idea that the probability of SRRC opening can be affected by and be proportional to SR Ca^{2+} load is supported by the work of Gyorke and Gyorke (1998). This type of functional linkage has been observed in both cardiac and skeletal muscle SR preparations (Gyorke and Gyorke, 1998; Ikemoto et al., 1989; Donoso et al., 1995; Lukyanenko et al., 1996; Sitsapesan and Williams, 1997), and in more detailed experiments (Ikemoto et al., 1989) there has been demonstrated a CSQ dependence for this interaction between luminal SR $[Ca^{2+}]$ and SRRC opening probability. Third, the concept that the Ca^{2+} buffering properties of CSQ might be influenced by the SRRC is consistent with the work of Ikemoto et al. (1991) and Gilchrist et al. (1992), where it was proposed that the opening of a threshold fraction of SRRCs is sufficient to elicit a reduction in CSQ Ca^{2+} affinity. This would have the effect of rapidly increasing the free $[Ca^{2+}]$ gradient across the junctional SR membrane and increasing the amount of luminal Ca^{2+} available for release into the fuzzy space. In our model, the Ca^{2+} affinity state of CSQ is linked to the binding of Ca^{2+} to the SRRC fast site, and the Ca^{2+} affinity of the SRRC slow site is linked to the binding of Ca^{2+} to CSQ. A detailed description of this element of regulation can be found in Appendix B. This mechanism is intuitively attractive because it lends a dynamic quality to a very large Ca^{2+} buffering "sink" that has been assumed by others to be governed by simple mass action.

Sarcoreticular Ca^{2+} cycling

The current model provides for Ca^{2+} diffusion from the fuzzy space to the sarcoplasm, taking into account Ca^{2+} buffers specific to each compartment. The predominant mechanism of Ca^{2+} removal from the sarcoplasm was assumed to be Ca^{2+} resequestration via the SR Ca^{2+}-ATPase. Aspects of this portion of the model that are worthy of note are the inclusion of a specific thermodynamic resequestration limit that accounts for the free $[Ca^{2+}]$ gradient between the SR lumen and the sarcoplasm (Shannon and Bers, 1997), CSQ as a luminal SR Ca^{2+} buffer that is subject to modulation by luminal and extraluminal influences (Gilchrist et al., 1992; Ikemoto et al., 1991), and an SR Ca^{2+} pump that operates via second-order reversible Michaelis-Menten kinetics. Ca^{2+} clearance from the sarcoplasm via cellular extrusion mechanisms, primarily via sodium-calcium exchange, was represented in a generalized form according to principles previously described by others (Philipson and Nishimoto, 1981; Reeves and Sutko, 1983; Tibbits et al., 1989).

Modeling methods

The mathematical representation of the Ca^{2+} regulatory mechanisms of a rat cardiac myocyte included a set of six differential equations with 33 parameter constants. The development of the differential equations is described in Appendix A. The input parameters are listed in Table 2. The derivation of the parameters from literature sources is explained in Appendix B. The set of differential equations was solved using a fourth-order Runge-Kutta numerical integration method. The required set of initial values was determined by solving for the model's self-defined steady state, analogous to quiescence. The quiescent state exhibited stable qualities consistent with those typically observed in isolated rat cardiac myocytes. For instance, it has been shown that the SR Ca^{2+} content does not undergo rest decay even after 5 min of quiescence (Bassani and Bers, 1995) and that resting $[Ca^{2+}]_c$ is quite stable (Satoh et al., 1997). For quiescence in the model, the differential equations were set to equal zero, the initial value of $[Ca^{2+}]_c$ was set to a baseline level (see Table 2 and Appendix B), and the set of equations and unknowns was solved using Newton's method for nonlinear algebraic equations, which generated the set of initial values used to solve the model. This method is important because the resting values of the processes and states (such as SR Ca^{2+} load, SRRC states, and membrane leaks) were not set, but rather were determined by the interactions of the modeled relationships.

To test the performance of the model, a series of experiments of varying complexity were simulated using two different approaches. First the model was tested in its ability to recapitulate the results of several previously published experiments (Bassani and Bers, 1995; Bassani et al., 1995; Bers et al., 1990; Cheng et al., 1996; Fabiato, 1985; Gilchrist et al., 1992; Ginsburg et al., 1998; Shannon and Bers, 1997; Wier et al., 1994). In these simulations, model parameters were varied to simulate the actual experimental interventions while the other model parameters were held constant. Second, in a subsequent set of simulations, model parameters were left unaltered and allowed to respond to a variety of contraction frequency manipulations. This provided an opportunity to determine if the model could reasonably simulate rest potentiation, frequency-dependent alterations in $[Ca^{2+}]_c$, and extrasystolic potentiation.

Experimental methods: $[Ca^{2+}]_c$ transients

Cardiac myocytes were obtained from the left ventricle (septum + free wall) of female Sprague-Dawley rats (Moore et al., 1991). In electrically paced cardiocytes, $[Ca^{2+}]_c$ transients were estimated using fura-2 fluorescence and ratiometric methods that have previously been described in detail (Palmer et al., 1999a; Szmacinski and Lakowicz, 1995). The data for the $[Ca^{2+}]_c$ dynamics were analyzed using custom-made software to determine the integral as well as the general magnitude and temporal characteristics for each $[Ca^{2+}]_c$ transient (Palmer et al., 1999b).

For the extrasystolic potentiation experiments, a pacing frequency of 1 or 2 Hz was used with a 2-s rest interval inserted within the pacing protocol. Potentiation was defined as the percentage increase in the integral of the post-rest-interval $[Ca^{2+}]_c$ transient relative to the mean integral of the normally paced $[Ca^{2+}]_c$ transient.

For the comparison of experimental versus simulated $[Ca^{2+}]_c$ transients, a representative $[Ca^{2+}]_c$ transient was generated using an interpolation scheme with the mean characteristics of a series of $[Ca^{2+}]_c$ transients from six myocytes paced at 0.25 Hz. The model was fit to the representative $[Ca^{2+}]_c$ transient, using an iterative least-squares fit algorithm. The parameter values estimated during the fit were the fura-2 concentration and

TABLE 2 The input: model parameters, definitions, values, and literature-based values. Refer to Appendix B for explanations. It is important to note that the values were converted to be representative of a nonmitochondrial and a nonsarcomeric protein cell volume

Parameter	Definition	Units	Model value	Literature-based value(s)
R_t	SRRC concentration	M	1.5×10^{-7}	1.5×10^{-7}
V_f	Volume fraction, fuzzy space	—	0.0013	0.0013 (<0.0019)
V_s	Volume fraction, SR	—	0.07	0.07 (i.e. 0.035/0.5)
V_c	Volume fraction, cytosol	—	0.9287	0.9287 ($1 - V_f - V_s$)
K_1	k_{off1}/k_{on1}, SRRC, fast site	M	7.0×10^{-7}	7.0×10^{-7}, (3.0×10^{-7} to 7.0×10^{-7})
K_2	k_{off2}/k_{on2}, SRRC, slow site	M	3.0×10^{-7}	3.0×10^{-7}, (3.0×10^{-7} to 7.0×10^{-7})
k_{on1}	Binding rate constant, SRRC, fast site	$(M \cdot s)^{-1}$	2.0×10^{9}	(1.0×10^{6} to 3.0×10^{9})
k_{on2}	Binding rate constant, SRRC, slow site	$(M \cdot s)^{-1}$	1.3×10^{7}	(1.0×10^{6} to 3.0×10^{9})
n_1	Hill coefficient, fast site	—	2	2
n_2	Hill coefficient, slow site	—	1	1
k_s	Release rate constant, SRRC	s^{-1}	9	1 to 12, (1 to 139)
k_l	Net L-type rate constant	s^{-1}	0.2	0.05 to 0.6
period	Period of Ca^{2+} influx	s	0.02	0.02
$V_{max,NaCaX}$	Maximum rate of Na^+/Ca^{2+} exchange	M/s	1.2×10^{-3}	1.2×10^{-3}
$K_{m,NaCaX}$	Dissociation constant, Na^+/Ca^{2+} exch.	M	3.6×10^{-5}	3.6×10^{-5}, (1.0×10^{-6} to 2.0×10^{-4})
n_{NaCaX}	Hill coefficient, Na^+/Ca^{2+} exchange	—	1	1
$V_{max,s}$	Maximum uptake rate, SR Ca^{2+}-ATPase	M/s	5.25×10^{-4}	(3.6×10^{-4} to 6.3×10^{-4})
$K_{m,s}$	Dissociation constant, SR Ca^{2+}-ATPase	M	2.5×10^{-7}	(2.0×10^{-7} to 8.3×10^{-7})
n_s	Hill coefficient, SR Ca^{2+}-ATPase	—	2	2
k_f	Diffusion rate constant, fuzzy space/cytosol	s^{-1}	2.5×10^{3}	(1.7×10^{3} to 2.0×10^{4})
$[Ca^{2+}]_e$	Extracellular free Ca^{2+} concentration	M	0.002	0.002
$B_{max,c}$	Maximum free fast buffers, cytosol	M	1.2×10^{-4}	(8.6×10^{-5} to 2.0×10^{-4})
$K_{b,c}$	Buffer dissociation constant (fast), cytosol	M	9.6×10^{-7}	9.6×10^{-7}
$[dye]_c$	Concentration of dye indicator, cytosol	M	—	Depended on experiment (see Materials and Methods)
$K_{b,dye}$	Dye indicator dissociation constant, cytosol	M	—	Depended on experiment (see Materials and Methods)
$B_{max,f1}$	Maximum free buffer, fuzzy space, site 1	M	2.0×10^{-4}	2.0×10^{-4}
$K_{b,f1}$	Buffer dissociation constant, fuzzy space, 1	M	1.1×10^{-3}	1.1×10^{-3}
$B_{max,f2}$	Maximum free buffer, fuzzy space, site 2	M	1.7×10^{-5}	1.7×10^{-5}
$K_{b,f2}$	Buffer dissociation constant, fuzzy space, 2	M	1.3×10^{-5}	1.3×10^{-5}
$B_{max,s}$	Maximum free buffer, SR	M	0.008	(0.005 to 0.014)
$K_{b,s}$	Buffer dissociation constant, SR	M	0.000638	0.000638
$k_{on,s}$	Buffer binding rate constant	$(M \cdot s)^{-1}$	8772	8772
$[Ca^{2+}]_c$	Quiescent free $[Ca^{2+}]$, cytosol	M	1.0×10^{-7}	1.0×10^{-7}, (4.0×10^{-8} to 1.6×10^{-7})

dissociation constant, both of which underwent an adjustment of less than 1%.

RESULTS

SR load depends on $[Ca^{2+}]_s$ limitations on uptake, $[Ca^{2+}]_c$, and SRRC leak

One unique feature of this model was the inclusion of a maximum theoretical thermodynamic gradient that can exist between the SR lumen and the sarcoplasm. Shannon and Bers (1997) clamped sarcoplasmic $[Ca^{2+}]$ ($[Ca^{2+}]_c$), using isolated SR microsomes from rat cardiac tissue, to demonstrate that under conditions where the SRRCs were blocked to prevent SR Ca^{2+} leak, SR luminal $[Ca^{2+}]$ ($[Ca^{2+}]_s$) varied linearly in proportion to changes in $[Ca^{2+}]_c$. The slope of this relationship, which was found to be ~7000 ($[Ca^{2+}]_s/[Ca^{2+}]_c$), was described as being representative of the concentration gradient that the SR Ca^{2+}-ATPase was able to produce given the free energy that would be expected to be available from ATP (Shannon and Bers, 1997). In a simple simulation of this experiment, model parameters were adjusted to represent the actual experimental interventions (SRRCs blocked and $[Ca^{2+}]_c$ varied) that were used by Shannon and Bers (1997). The results of this simulation are found in Fig. 2 *A*. It is not at all surprising that this simple simulation recapitulated a slope of 7000 ($[Ca^{2+}]_s/[Ca^{2+}]_c$) because this concept was built into our model.

More important, however, is the model prediction of the Ca^{2+} gradient that should exist between the sarcoplasm and the SR lumen under normal conditions. Simulating the above experiment without SRRC blockade resulted in lower levels of SR Ca^{2+} load (Fig. 2 *A*). For instance, at $[Ca^{2+}]_c = 1 \times 10^{-7}$ M, the gradient was 3011 ($[Ca^{2+}]_s/[Ca^{2+}]_c$) (see Table 3), in comparison to the value of ~7000 ($[Ca^{2+}]_s/[Ca^{2+}]_c$) with the SRRC blocked.

SRRC leak

There are currently several distinctly different viewpoints regarding the relative importance of SRRC Ca^{2+} leak and SR Ca^{2+} uptake (and "back-flux"; see next paragraph) in

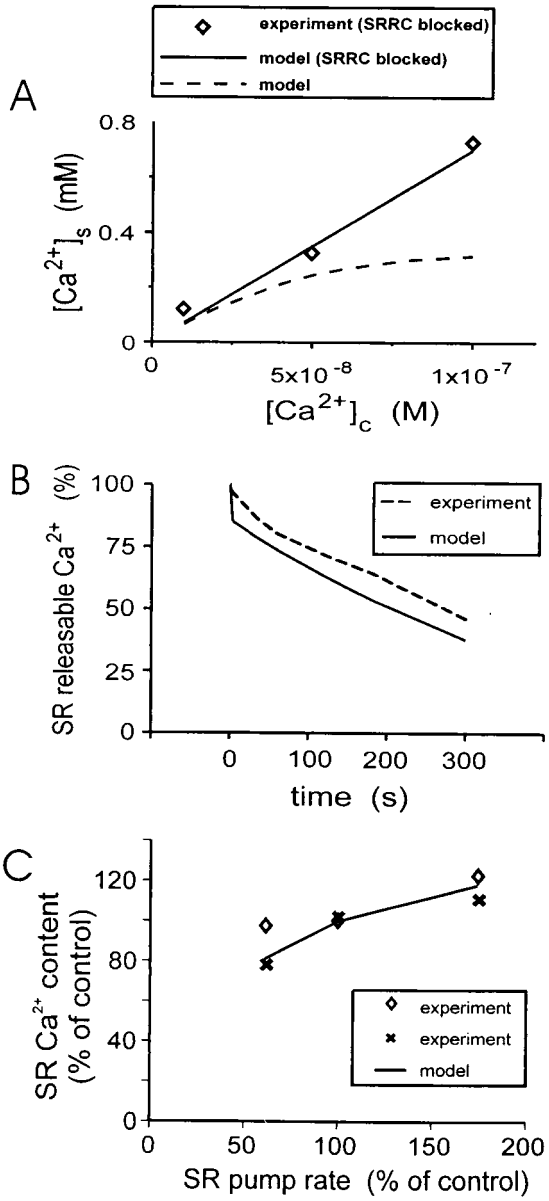

FIGURE 2 (*A*) The thermodynamic gradient. Shannon and Bers (1997) used cardiac microsomes with entrapped furaptra in experiments designed to examine the ability of the SR to take up Ca^{2+} relative to $[Ca^{2+}]_c$. The SRRCs were blocked with ruthenium red (20 μM). There was an observable gradient (~7000 ($[Ca^{2+}]_s/[Ca^{2+}]_c$)) between the SR and the cytosol when the SRRCs were blocked. The experimental data (◇) are from Shannon and Bers (1997) with permission. The model (——) simulated the gradient (slope = 7000 ($[Ca^{2+}]_s/[Ca^{2+}]_c$)). To simulate this protocol the following were performed: 1) the parameter for the SRRC release rate constant, k_s, was set to zero (to block the SRRC), 2) the value for the variable representing $[Ca^{2+}]_c$ was set (to vary $[Ca^{2+}]_c$), 3) the variable for $[Ca^{2+}]_s$ was solved for (to measure $[Ca^{2+}]_s$), and 4) all other parameters were held constant. The model also provided a prediction of the gradient in a normal cell, i.e., no blocking of the SRRC (- - - -). Note that in contrast to the other experimental simulations, the dye indicator that was applied to the SR in the experiment was not represented in the model. The current version of the model was not designed to represent dye indicators in the SR. In the case of this experiment, the deletion should not be of much concern, because the generated gradient was relative to the free SR $[Ca^{2+}]$ at equilibrium conditions. (*B*) SR leak. To estimate the SR Ca^{2+} leak rate, Bassani and Bers (1995) used quiescent cells with SR uptake blocked and Na^+-Ca^{2+} exchange enhanced to measure the time-dependent depletion of caffeine-releasable SR Ca^{2+} (- - - -); data were replotted with permission. A simulation of this protocol was performed using the following interventions: 1) set $V_{max,s} = 0$ (to block SR uptake), 2) set $K_{m,NaCaX} = 3 \times 10^{-6}$ (to enhance Na^+-Ca^{2+} exchange), 3) solve for releasable SR Ca^{2+} over time (——), where the maximum releasable Ca^{2+} was determined to be 60% of the load in the normal quiescent state, and 4) solve for SR leak rate through the SRRCs. (*C*) SR pump rate and SR Ca^{2+} load. Ginsburg et al. (1998) used pharmacological interventions to adjust the SR pump rate, and the effect on SR Ca^{2+} content was determined (×, ◇). Data are reproduced from the *Journal of General Physiology*, 1998, 111:491–504, by copyright permission of the Rockefeller University Press. In the model simulation (——), $V_{max,s}$ was adjusted to match the apparent experimental 39% decrease and 74% increase in SR pump rate.

determining SR Ca^{2+} content. In our model, SRRC leak plays a major role. Our model produced a value of 0.06 mM/s for the leak of Ca^{2+} through open SRRCs during a simulated state of quiescence that compares favorably to a theoretical estimate (0.02 mM/s) reported by Wier et al. (1994) for similar experimental conditions. However, these values are approximately two orders of magnitude higher than an experimentally determined diastolic Ca^{2+} leak estimate (0.3 μM/s) reported by Bassani and Bers (1995). The lower leak estimate was derived under experimental conditions where SR Ca^{2+} uptake was blocked and forward Na^+-Ca^{2+} exchange was markedly stimulated, whereas the higher leak values were derived from theoretical estimates under conditions where SR Ca^{2+} uptake and Na^+-Ca^{2+} exchange were unaltered. In our model, when SR Ca^{2+} uptake was blocked and Na^+-Ca^{2+} exchange was accelerated, there was a rapid reduction in the predicted diastolic SRRC Ca^{2+} release rate to 0.24 μM/s, and the subsequent time-dependent decline in releasable SR Ca^{2+} content was strikingly similar to that observed by Bassani and Bers (1995) (Fig. 2 *B*). The theoretical reduction in SRRC leak rate elicited by SR pump blockade and Na^+-Ca^{2+} exchange acceleration occurred secondary to a reduction in fuzzy space $[Ca^{2+}]$ and, to a lesser extent, a reduction in SR Ca^{2+} load. Finally, it should be recognized that the magnitude of the hypothetical leak reduction predicted by our model is less important than the general concept that SRRC Ca^{2+} leak rate and sarcoreticular Ca^{2+} regulation can be markedly affected by experimental intervention, an issue that will be addressed in the Discussion.

Recently, a very interesting hypothesis has been advanced that "SR pump back-flux" is the primary determinant of SR Ca^{2+} content, whereas SRRC Ca^{2+} leak plays only a minor role (Ginsburg et al., 1998; Shannon et al., 2000). Ginsburg et al. (1998) found that in isolated cardiocytes when SR Ca^{2+} uptake was increased by 74% or decreased by 39%, SR Ca^{2+} content was increased by ~10–20% or decreased by 5–23%, respectively (Fig. 2 *C*).

TABLE 3 The output: model predicted values for the $[Ca^{2+}]_c$ transient in Fig. 5, compared to experimental values. Values have been converted to be representative of a nonmitochondrial and a nonsarcomeric protein cell volume (see Appendix B).

Definition	Units	Predicted value	Converted experimental value(s)	References
SR Ca^{2+} content	μM	201	182, (119 to 840)	a,b,c
SR Ca^{2+} fractional release*	%	60	55.4 (35 to 60)*	a,c
Gradient, (free) $[Ca^{2+}]_s$ vs. $[Ca^{2+}]_c$ at steady state	—	3011	$\leq$7000	d
Ca^{2+} influx, maximum	mM/s	0.4	$\sim$0.25 to 0.4	e,f
SR Ca^{2+} release, maximum	mM/s	3.3	$\geq$2, 3.2 to 11.4	g,e
Gain, (Ca^{2+} release,max./Ca^{2+} influx,max.)	—	8.3	$\leq$16	f
Ca^{2+} influx, flux integral	μM	8.6	6.2 to 9.0	a,h
SR Ca^{2+} release, flux integral	μM	120.5	77 to 134	a,b
Total Ca^{2+} delivery	μM	129.1	$\sim$126.1 for $[Ca^{2+}]_c = 1$ μM	i
Ca^{2+} influx, % of Ca^{2+} delivery	%	6.7	7 to 8	e,a
SR Ca^{2+} release, % of Ca^{2+} delivery	%	93.3	$\sim$92 to 93	a,e
$[Ca^{2+}]_c$, peak	μM	1.16	$\sim$1 μM for $\sim$126 μM Ca^{2+} delivery	b
Time constant of $[Ca^{2+}]_c$ decline, τ	ms	160	191 when peak $[Ca^{2+}]_c = 1$ μM	j
Buffer power (total Ca^{2+} delivery/$\Delta[Ca^{2+}]_c$)	—	122	110.3 $\pm$ 16.5	k
Cytosol buffer, % Ca^{2+} free vs. bound, peak	%	0.97	$\sim$1	e,g
SR buffer, % Ca^{2+} free vs. bound, steady state	%	10.5	$\leq$10	d,l
SR free $[Ca^{2+}]$ at steady state	mM	0.30	0.35 to 0.50	d
Time to peak $[Ca^{2+}]_c$	ms	60	25 to 81	m,n,o,p,q
Max. rate of rise of $[Ca^{2+}]_c$, total	mM/s	3.7	$\geq$2.8	b
Max. rate of rise of $[Ca^{2+}]_c$, free	mM/s	0.036	0.008 to 0.034	m,n,r
Time to 25% return	ms	53	77 $\pm$ 8	s
Time to 50% return	ms	113	147 $\pm$ 22	s
Time to 75% return	ms	228	278 $\pm$ 42	s
Time to 90% return	ms	393	613 $\pm$ 164	s
SR Ca^{2+}-ATPase, flux integral (net)	μM	115.3	$\sim$77 to 134 (i.e. $\sim$same as SR Ca^{2+} release)	b
Na^+-Ca^{2+} exchange, flux integral	μM	9.0	$\sim$6.2 to 9.0 (i.e. $\sim$same as Ca^{2+} influx)	b
SR Ca^{2+}-ATPase, % of total Ca^{2+} removal	%	92.8	91 to 97	t,u,v
Na^+-Ca^{2+} exchange % of total Ca^{2+} removal	%	7.2	3 to 9	t,u,v
Total Ca^{2+} removal (net)	μM	124.3	$\sim$126.1 (i.e. $\sim$same as Ca^{2+} delivery)	b
Fraction: Ca^{2+} delivery/Ca^{2+} removal	—	1.04	1, (when influx = efflux)	b
SR Ca^{2+} leak (quiescent)	mM/s	0.06	0.02, (quiescent)	f
SR Ca^{2+} leak (with interventions†)	μM/s	0.24	0.3, (with interventions)†	w
Fuzzy space $[Ca^{2+}]$, peak	μM	1.8	2.3, 2 to 3 for max. activation	x,y
Fuzzy space $[Ca^{2+}]$, baseline	μM	0.12	Unknown	—
SRRC r_o, maximum	—	0.53	Unknown	—
SRRC r_o, baseline	—	0.02	Unknown	—
SRRC $r_r + r_c$, maximum	—	0.81	Unknown	—
SRRC $r_r + r_c$, baseline	—	0.29	Unknown	—

*SR uptake blocked.

†Na^+-Ca^{2+} exchange enhanced and SR uptake blocked.

[a]Delbridge et al., (1997). For a review see [b]Bers (1993), [c]Bassani et al. (1995), [d]Shannon and Bers (1997), [e]Sipido and Wier (1991), [f]Wier et al. (1994), [g]Berlin et al. (1994), [h]Yuan et al. (1996), [i]Hove-Madsen and Bers (1993), [j]Bers and Berlin (1995), [k]Delbridge et al. (1996), [l]Ikemoto et al. (1989), [m]Moore et al. (1991), [n]Moore et al. (1993), [o]Konishi and Berlin (1993), [p]Palmer et al. (1999a), [q]Palmer et al. (1999b), [r]Janczewski et al. (1995), [s]unpublished data from our laboratory experiments, [t]Li et al. (1998), [u]Bassani et al. (1994), [v]McCall et al. (1998), [w]Bassani and Bers (1995), [x]Sham et al. (1995), [y]Fabiato (1985).

These data were interpreted as being supportive of SR pump back-flux. Our model does not incorporate the back-flux concept per se, but rather uses a representation of net forward SR Ca^{2+} pump rate that is subject to regulation by SR luminal and cytosolic $[Ca^{2+}]$. However, when we simulated the SR Ca^{2+} uptake rate interventions used by Ginsburg et al. (1998), SR Ca^{2+} content increased by 18% or decreased by 19% in response to a 74% increase or a 39% decrease in SR Ca^{2+} uptake rate, respectively (Fig. 2 *C*). These simulated SR Ca^{2+} content changes are comparable to those observed by Ginsburg et al. (1998). These results indicate that the findings of Ginsburg et al. (1998) can also be explained by a regulatory scheme in which SRRC Ca^{2+} leak is more dominant in determining SR Ca^{2+} content.

The above findings are particularly relevant in our model for several reasons. First, examination of the theoretical processes that give rise to this finding provides insight into the relative importance of SR Ca^{2+} uptake and leak in determining SR Ca^{2+} load. Second, this in turn is very important in view of the fact that bidirectional interactions between the Ca^{2+} load in the SR lumen and the SR Ca^{2+} release channels provide robust control of cellular Ca^{2+}

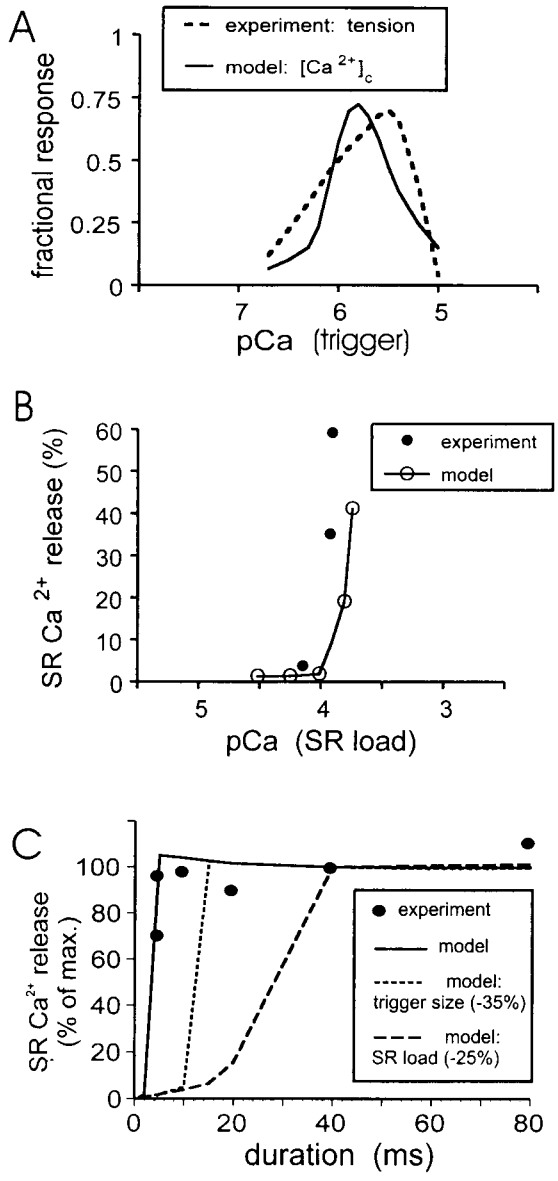

FIGURE 3 (*A*) The graded response. Reconstruction of data from Fabiato (1985) displaying the relationship between the fraction of maximum tension and pCa (trigger Ca^{2+}), using skinned canine Purkinje fibers (- - - -). Reproduced from the *Journal of General Physiology*, 1985, 85: 247–289, by copyright permission of the Rockefeller University Press. In the actual experiment, pCa changes were effected rapidly (ms), and the resulting tension was measured. Developed tension was interpreted to be an indirect metric of SR Ca^{2+} release. There were observable activation and inactivation effects with Ca^{2+} release relative to the size of the Ca^{2+} trigger. The model simulated similar activation and inactivation effects due to Ca^{2+} trigger size (——), as indicated by peak $[Ca^{2+}]_c$ as a fraction of maximum. To produce the simulation of this protocol, the following interventions were performed: 1) set the value for the $[Ca^{2+}]$ to which the SRRC were exposed (to vary $[Ca^{2+}]$ in the external solution), 2) effect a rapid (1 ms) change in the trigger $[Ca^{2+}]$, 3) solve for the peak $[Ca^{2+}]_c$ as a fraction of the $[Ca^{2+}]_c$ following complete SR Ca^{2+} release. For the simulation, it was assumed that skinned Purkinje fibers would not have the structural architecture necessary for tightly confined fuzzy space regions (there would be no t-tubules and the sarcolemma would be compromised). Therefore, the fuzzy space was modeled to be continuous with the cytosol by an increase in the diffusion rate constant to 3500 s^{-1}. All other parameters were held constant. (*B*) Load dependence of SR Ca^{2+} release. Bassani et al. (1995) produced the data (●) (replotted by permission), using isolated ferret cardiocytes. To perform this simulation (——), SR loading was varied by using the above thermodynamic gradient protocol (without SRRC blockade). The L-type channel rate constant, k_1, was briefly increased to trigger SR Ca^{2+} release. (*C*) Effect of trigger duration on SR Ca^{2+} release. Bers et al. (1990) estimated the data (●) (reconstructed with permission), using isolated rat cardiocytes. The simulation (——) was performed by varying period and providing a k_1 trigger. In addition, simulations were performed with reduced trigger rate (k_1 decreased by 35%) (·····) and reduced SR load (−25%) (- - - -), using the loading scheme of Fig. 2 *A*. All data were normalized as a percentage of the SR Ca^{2+} release with a 40-ms duration.

dynamics under a variety of more sophisticated experimental simulations.

SR Ca^{2+} release depends on SR load, SRRC recovery, and Ca^{2+} trigger size and duration

Graded response

A characteristic that is assumed to be fundamental to cardiac muscle CICR is that the amount of Ca^{2+} that is released from the SR varies or is graded as a function of the trigger $[Ca^{2+}]$ (Gyorke and Gyorke, 1998; Fabiato, 1985). In the classic work of Fabiato (1985), the relationship between the trigger $[Ca^{2+}]$ (pCa) and the response (tension) had the following characteristics: 1) a threshold pCa ($\sim >7$) at which initial tension development was elicited; 2) a "graded response" that increases when pCa is increased until a maximum response is achieved (pCa $\approx$ 5.5); 3) a progressive inactivation of the response that occurs with further increases in trigger $[Ca^{2+}]$ (see Fig. 3 *A*). In Fabiato's experiments (Fabiato, 1985), it was assumed that the tension response was reflective of a graded CICR response. This assumption is supported by the work of Gyorke and Gyorke (1998), who demonstrated similar characteristics when the response metric was the cardiac SRRC channel open probability in planar bilayer preparation. Kim et al. (1983) observed similar results when measuring Ca^{2+} release rates from isolated skeletal SR vesicles.

As can be seen in Fig. 3 *A*, the simulation of this "graded response" experiment produced a pCa-response (peak $[Ca^{2+}]_c$) relationship with qualities of a threshold, a graded response, and inactivation that were similar to those observed by Fabiato (1985). While it is clear from inspection of Fig. 3 *A* that the model prediction and the experimental data of Fabiato (1985) are not perfectly superimposable, it is important to note that the general pattern of the modeled graded response was reasonably similar to that observed experimentally. The reasons for this divergence will be addressed in the Discussion.

Load dependence of SR Ca^{2+} release

It has been clearly demonstrated that SR Ca^{2+} load has a distinct effect on the SR Ca^{2+} release (Gilchrist et al., 1992; Bassani et al., 1995). Specifically, SR Ca^{2+} release cannot be induced until a threshold level of SR loading is reached, after which SR Ca^{2+} release demonstrates a steep SR Ca^{2+} load dependence. This effect should be present in the model with the inclusion of the SRRC-CSQ bidirectional feedback. To test this, the loading scheme of Fig. 2 *A* was used (with no blocking of the SRRC), and a release trigger was provided at various SR Ca^{2+} loads. The results of this protocol (Fig. 3 *B*) demonstrate a threshold followed by a steep load dependence of SR Ca^{2+} release, as has previously been demonstrated (Bassani et al., 1995).

Effect of Ca^{2+} trigger duration on SR Ca^{2+} release

CICR has been demonstrated to be independent of Ca^{2+} trigger duration at periods greater than 5 ms (Fig. 3 *C*) (Bers et al., 1990; Cannell et al., 1987). The model reproduces this relationship and predicts the occurrence of a graded response at durations of less than 5 ms (Fig. 3 *C*). More recent studies have found that the range of durations that produce a graded response is extended after reductions in SR Ca^{2+} loading or maximum Ca^{2+} influx (trigger size) (Han et al., 1994; Isenberg and Han, 1994; Spencer and Berlin, 1995). With the simulation of a 35% decrease in trigger rate or a 25% decrease in SR Ca^{2+} load, duration-dependent gradedness is predicted to occur with trigger durations less than 15 ms or less than 40 ms, respectively (Fig. 3 *C*).

Time-dependent recovery of SR Ca^{2+} release

This simulation was designed to resemble a study (Cheng et al., 1996) where in discrete spaces (in which "sparks" were observable) $[Ca^{2+}]$ was monitored during the course of a spontaneous SR Ca^{2+} release and during a subsequent stimulated SR Ca^{2+} release that was invoked at variable times after the spontaneous event. The level of the second stimulated SR Ca^{2+} release increased with the amount of recovery time, eventually approaching the original level of the spontaneous release (see Fig. 4 *A*). Cheng et al. (1996) suggested that this pattern was representative of a refractory state of the cell's ability to release Ca^{2+}. The model simulation of the experiment (see Fig. 4 *B*) closely resembled the time-dependent recovery pattern observed by Cheng et al. (1996).

The utility of the simulated experiment is that it provides one with a glance at the cellular events that are hypothetically associated with this time-dependent recovery process. For example, in our simulation, it appears that repletion of SR Ca^{2+} load was occurring early on in the time-dependent recovery of SR Ca^{2+} release, whereas SRRC state shifts from "refractory" and "closed" states to the "activatable"

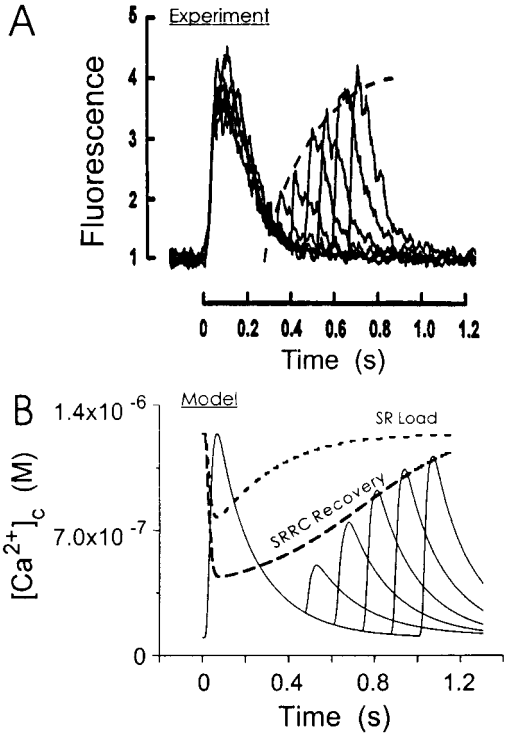

FIGURE 4 The time-dependent recovery of SR Ca^{2+} release. In *A* (with permission) is a figure from Cheng et al. (1996), who observed fluo-3 fluorescence changes (relative to $[Ca^{2+}]$) in confined spaces in which Ca^{2+} sparks were observed. There was a time-dependent recovery of the ability to release Ca^{2+}, indicated by the dashed line. In *B*, the model simulated this time-dependent recovery of SR Ca^{2+} release. For comparison, the time course of the recovery of total $[Ca^{2+}]_s$ (- - - -) has been scaled and superimposed on *B*. The model predicted that the total $[Ca^{2+}]_s$ was almost fully recovered before the recovery of SR Ca^{2+} release was complete. Furthermore, the time course of the recovery of the SRRC from inactivation has been represented by the inverse of the sum of the fractions of the SRRC in the closed and the refractory states $(1/(r_c + r_o))$. The SRRC recovery (– – –) was scaled and superimposed on *B*. The model predicted that the major source of refractoriness would be inherent in the SRRC. The experiment was modeled using the following steps: 1) the L-type channel rate constant, k_1, was briefly increased to trigger a SR Ca^{2+} release, and 2) the time interval between triggered Ca^{2+} releases was varied. $[Ca^{2+}]_c$ was solved for the time course of the simulation. Summary of parameter changes: 1) k_1 underwent a brief step change; 2) the dye indicator was fluo-3: $[\text{fluo 3}]_c = 5 \times 10^{-5}$ M and $K_d = 1.13 \times 10^{-6}$ M (Smith et al., 1998); 3) all other parameters were held constant.

state occurred throughout the recovery process (Fig. 4 *B*). The simulation suggests that refractoriness inherent to the SRRCs is the dominant factor and that restoration of SR Ca^{2+} load is only a modest factor in the time-dependent recovery of SR Ca^{2+} release.

Model response to alterations in contraction frequency

As mentioned earlier concerning the types of experiments that will be described in the following text, model param-

eters were not manipulated but simply allowed to respond to the delivery of periodic contraction stimuli. It is important to note that the model parameter values that were used all fell within value ranges that have been reported in the literature (Table 2). Using these values, we found that the simulated $[Ca^{2+}]_c$ transient displayed characteristics that were very similar to those observed in the laboratory with fura-2 fluorescence (Fig. 5). In the "stimulated" generation of a simulated $[Ca^{2+}]_c$ transient, we manipulated a single external control point, perturbing the model from its self-determined steady state. The model equations responded to this perturbation, producing a $[Ca^{2+}]_c$ transient *en route* to a new steady state. Because the model equations were concentration driven, all of the underlying Ca^{2+} regulatory processes were not defined but predicted and could be quantified and compared to literature results (Table 3).

As constructed, the model demonstrates appropriate Ca^{2+} delivery qualities that are consistent with our understanding of these properties from the literature. In particular, the bidirectional control loop between the SRRCs and CSQ (the SR luminal Ca^{2+} sensor element) was fundamentally important in the ability of the model to exhibit reasonable SRRC gain, fractional Ca^{2+} release from the SR, as well a proper rate of rise and time-to-peak $[Ca^{2+}]_c$. With regard to these latter features, it should be noted that in generating the simulated $[Ca^{2+}]_c$ transient, we included Ca^{2+} buffering by fura-2 in the model. Were it not for the inclusion of fura-2 buffering in the model, the simulated transients would have had different quantitative and temporal characteristics. In several of the experiments described below, it should be noted that simulated data include a fura-2 Ca^{2+} buffering element and are compared with actual experimental $[Ca^{2+}]_c$ data derived with fura-2 fluorescence.

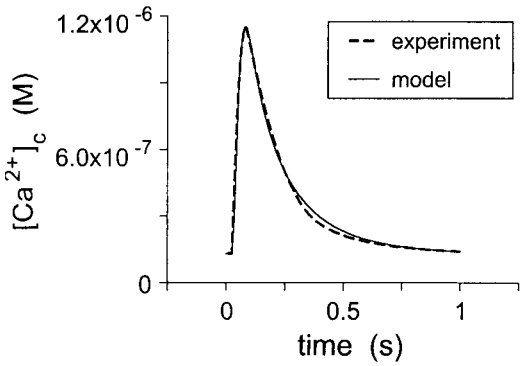

FIGURE 5 Comparison of a steady-state $[Ca^{2+}]_c$ transient generated at a low pacing frequency (0.25 Hz), produced by experiment (– – –) and model simulation (——). The associated model predictions of Ca^{2+} regulatory quantities are listed in Table 3. In this simulation, parameter changes included the following: 1) k_1 underwent brief step changes at 0.25 Hz; and 2) a dye indicator, fura-2, was included: $[\text{fura 2}]_c = 5 \times 10^{-5}$ M, $K_d = 2 \times 10^{-7}$ M (Grynkiewicz et al., 1985).

Rest potentiation

The simplest alteration in contraction frequency is when a myocyte makes the transition from quiescence to a fixed pacing frequency. Examples of simulated transitions from quiescence to steady-state contractile activity are depicted in Fig. 6, *A* and *B*. The model output yields a relatively large initial $[Ca^{2+}]_c$ followed by a rapid progression to a reasonably stable steady state. This behavior is strikingly similar to what is observed in the laboratory with isolated rat cardiocytes, and the initial response represents "rest potentiation." Based on the model predictions, the larger initial response would be predominantly due to greater SRRC recovery from inactivation at the time of the first stimulation relative to that of the ensuing stimulations. The pacing rate allowed for 1 s (Fig. 6 *A*) or 0.5 s (Fig. 6 *B*) of recovery time between stimulations. The model predicts that after 1 s, SR Ca^{2+} reuptake would be virtually completed, yet the SRRCs would not be entirely recovered from inactivation (Fig. 6, *C–F*). Variable $[Ca^{2+}]_c$ transients occurred until the SRRC activation-inactivation cycle settled into a dynamic steady state. The SR Ca^{2+} load was predicted to remain relatively unchanged with alterations in pacing frequency, as was observed experimentally (Bouchard and Bose, 1989).

Negative staircase

Mammalian cardiocytes are known to be sensitive to alterations in contraction frequency, and in the case of rat ventricular myocytes, they display a negative force versus frequency response (Bers, 1993). Using our model, when the pacing frequency of a simulated rat cardiocyte is increased, the amplitude of the $[Ca^{2+}]_c$ response decreases (Fig. 6 *G*). When the model was run at a variety of pacing frequencies that are typically used in the laboratory, a peak $[Ca^{2+}]_c$ versus pacing frequency relationship was produced (Fig. 6 *H*). These simulated effects of pacing frequency are strikingly similar to those observed in the laboratory (Bers, 1989).

Extrasystolic potentiation

Once the model demonstrated the capacity to predictably simulate steady-state frequency responses, we investigated the ability of the model to accommodate a dynamic pacing frequency perturbation in the form of a delivered extrasystolic interval. In our simulations, steady-state pacing at two different frequencies was interrupted by the delivery of a 2-s extrasystolic interval, and the ensuing $[Ca^{2+}]_c$ transients were examined (Fig. 7, *A* and *B*). In both cases, the extrasystolic $[Ca^{2+}]_c$ response was potentiated and the potentiation was most robust when the extrasystolic interval was delivered at the higher pacing frequency. These simulated responses are strikingly similar to the responses observed in

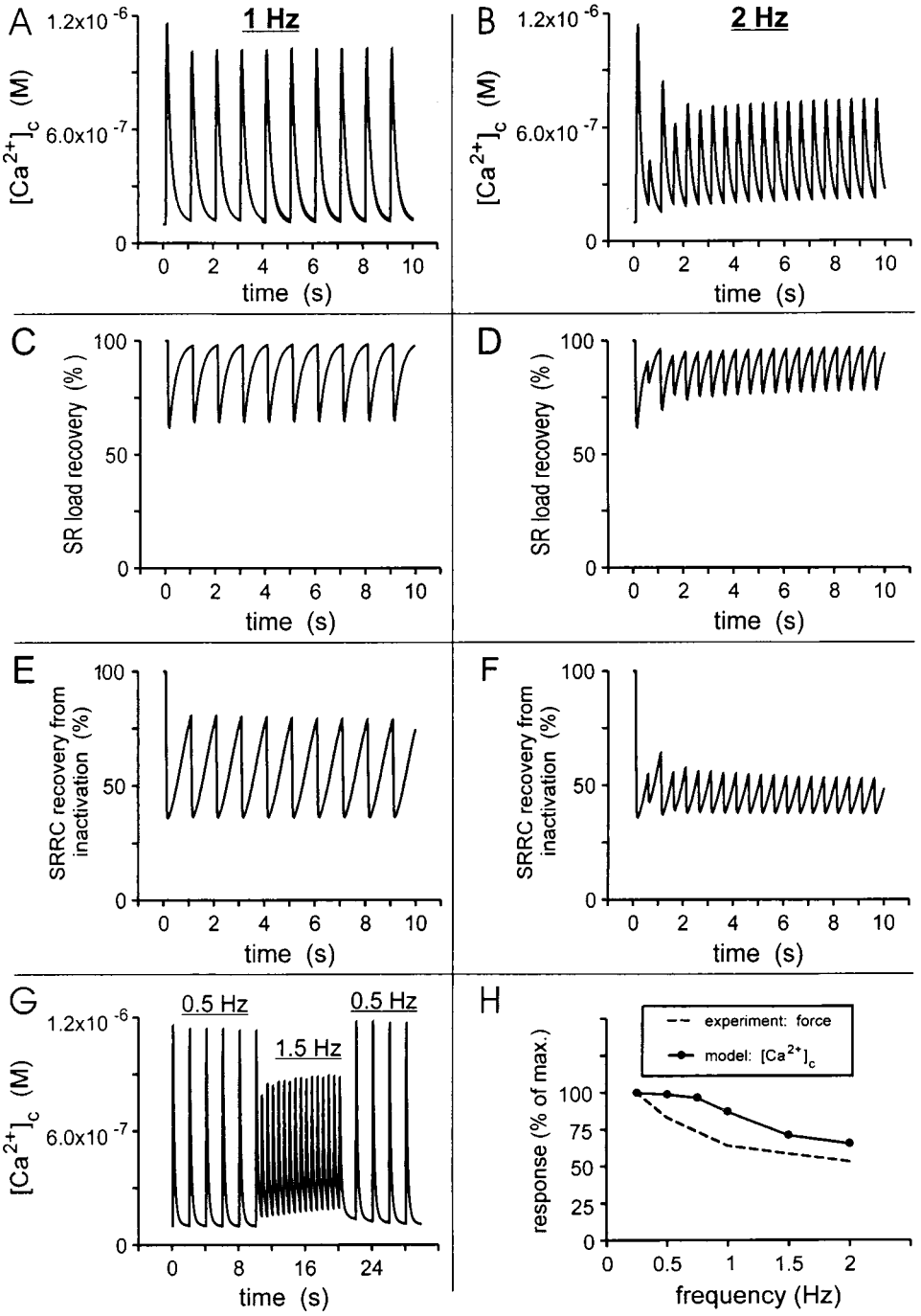

FIGURE 6 The frequency-dependent response of a modeled series of $[Ca^{2+}]_c$ transients initiated during quiescence. The pacing rate was varied: 1 Hz (*A*), 2 Hz (*B*), and 0.5/1.5/0.5 Hz (*G*). The time course of $[Ca^{2+}]_s$ (as a percentage of the baseline level) is shown for 1 Hz (*C*) and 2 Hz (*D*). The time course of the recovery of the SRRC from inactivation has been represented by the sum of the fractions of the SRRC in the closed and the refractory states ($r_c + r_o$) (as a percentage of the baseline level) for 1 Hz (*E*) and 2 Hz (*F*). In *H* is a summary of the effect of frequency on peak $[Ca^{2+}]_c$ (% of maximum) (——) with data from Bers (1989) (– – –) (used with permission). In the simulation, parameter changes included the following: 1) k_1 underwent brief step changes at variable frequencies; and 2) a dye indicator, fura-2, was included: $[\text{fura 2}]_c = 5 \times 10^{-5}$ M, $K_d = 2 \times 10^{-7}$ M (Grynkiewicz et al., 1985).

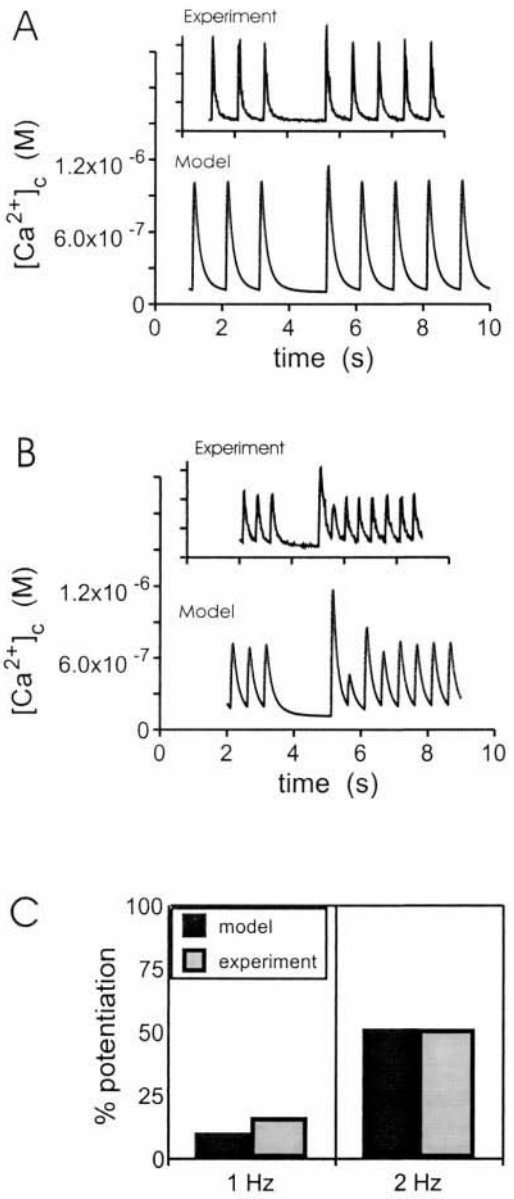

FIGURE 7 Extrasystolic potentiation responses from actual and simulated pacing experiments. A modeled series of $[Ca^{2+}]_c$ transients was generated with a 2-s extrasystolic interval within a background pacing rate of 1 Hz (*A*) and 2 Hz (*B*). Representative experimental results from individual cardiocytes (*A* and *B*, *inset*) compare favorably. Data in the inset are scaled for the purposes of comparison. The inset time axes are subdivided into 2-s increments. In *C* is a summary of the effect of pacing rate on extrasystolic potentiation, including a comparison of the model and the experimental results. Model parameter changes are analogous to those described in the legend of Fig. 6.

the laboratory (Fig. 7, *A* and *B*, *insets*; summarized in Fig. 7 *C*). An examination of the model output reveals that the basis for the extrasystolic response elicited at the 1- and 2-Hz pacing frequencies was largely due to the collective recovery of SRRCs to an activatable state.

Pulsus alternans

In a final simulation, cellular Ca^{2+} loading was invoked by suppressing Ca^{2+} efflux from the cell during pacing at 2 Hz. As can be seen in Fig. 8, the Ca^{2+} overload elicited an unstable and cyclic $[Ca^{2+}]_c$ transient irregularity that qualitatively resembled the phenomenon of pulsus alternans (Kihara and Morgan, 1991; Wong et al., 1992). In our model, the genesis of this phenomenon was due to control feedback instabilities in the bidirectional communication between SRRCs and CSQ, related to a disruption in the degree and timing of Ca^{2+} binding to the SRRC and CSQ during the cycling of control elements associated with a $[Ca^{2+}]_c$ transient. It is also important to note that large and relatively long-lived fluctuations in SR Ca^{2+} load or fuzzy space $[Ca^{2+}]$ were not necessary to generate this alternans effect.

DISCUSSION

Insights provided by model predictions

Graded response

The graded response is a fundamental cardiac physiological behavior that is sufficiently represented by our model (Fig. 3 *A*). Several regulatory features included in our model were important in conferring the properties of the graded response. The use of SRRCs with several Ca^{2+}-sensitive functional states and bidirectional modulatory interplay between SRRCs and Ca^{2+} buffering in the SR lumen were centrally important in this regard. An SRRC model where various functional states were governed by $[Ca^{2+}]$ in the fuzzy space was fundamental in our representation of the graded response. This type of Ca^{2+}-dependent regulation of SRRC kinetics (without a fuzzy space) has been described previously (Tang and Othmer, 1994) and was sufficient for the production of a graded response, albeit only in the context of SR Ca^{2+} release channel opening. While our

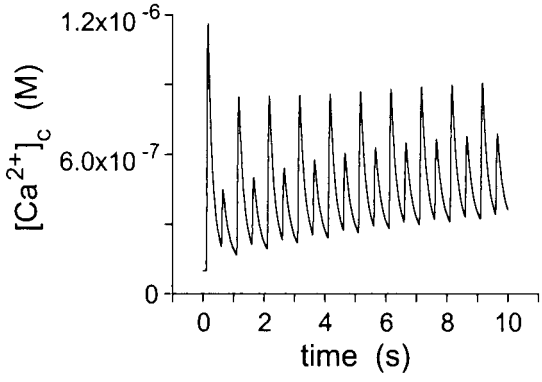

FIGURE 8 The simulated effect of Ca^{2+} overload on a series of $[Ca^{2+}]_c$ transients at a pacing frequency of 2 Hz. The outcome closely resembles the phenomenon of pulsus alternans (Kihara and Morgan, 1991).

scheme for the regulation of functional SRRC states via $[Ca^{2+}]$ changes in the fuzzy space was sufficient to confer a graded response behavior to the model, it was not adequate to provide for the proper amplification of the SR Ca^{2+} release response. We found that inclusion of bidirectional communication between the SRRC and Ca^{2+} sensing elements in the SR lumen was important for the replication of observed whole-cell responses. A system in which SRRCs were subject to control by events on either side of the SR terminal cisternal membrane, and in which luminal SR buffers were subject to modulation by SRRC functional status, was essential in controlling the quantity of and rate at which SR Ca^{2+} was released and in ensuring that Ca^{2+} release from the SR was graded or fractional as opposed to all or nothing. In addition, the bidirectional control element confers a more dynamic quality on luminal SR Ca^{2+} buffers and, therefore, the regulation of luminal SR $[Ca^{2+}]$.

Bidirectional communication between SRRCs and SR lumen Ca^{2+} sensing elements was not only critical in amplifying the SR Ca^{2+} release channel reaction to a whole-cell response; it was important in providing a tightly controlled mechanism for the cessation of SR Ca^{2+} release. The latter feature has been an issue that, until very recently, has been rather inadequately dealt with in most models of cardiocyte Ca^{2+} dynamics. A mechanism for a regulated termination of Ca^{2+} release is essential in a system displaying a graded response and fractional, rather than all-or-none, release of Ca^{2+} from the SR. In a recent modeling study by Rice et al. (1999) it was proposed that Ca^{2+} release termination could occur secondary to a transient local depletion of junctional SR Ca^{2+} during CICR. This scheme of local Ca^{2+} depletion requires the existence of two distinct pools of Ca^{2+} in the SR lumen: a junctional SR Ca^{2+} release pool and a SR Ca^{2+} uptake pool that ultimately replenishes the former pool when it is depleted. In this hypothetical mechanism, local depletion terminates SR Ca^{2+} release before large amounts of Ca^{2+} from the uptake pool can be made available for release in the release pool, thus ensuring that the SR Ca^{2+} release process is fractional rather than all or nothing. There is evidence, however, against such a discrete organization of Ca^{2+} pools in the SR lumen (Sham et al., 1998; Satoh et al., 1998).

Alternatively, it has been argued that if the SR is treated as a single Ca^{2+} pool, a Ca^{2+} depletion-induced termination of Ca^{2+} release would require a nearly complete emptying of SR Ca^{2+}; this does not occur (Delbridge et al., 1997; Bassani et al., 1995). Complete emptying of a single-pool SR need not occur in a system where SRRCs and CSQ are functionally coupled. It is now known that cardiac SRRCs and CSQ are physically coupled by junctin and triadin (Zhang et al., 1997) and that SR Ca^{2+} release and SRRC activatability are strongly influenced by SR Ca^{2+} content (Bassani et al., 1995; Donoso et al., 1995; Gyorke and Gyorke, 1998; Gilchrist et al., 1992; Ikemoto et al., 1989; 1991; Janczewski et al., 1995; Lukyanenko et al., 1996; Satoh et al., 1997; Shannon and Bers, 1997; Sitsapesan and Williams, 1997). In fact, it has been demonstrated that in systems absent of CSQ, Ca^{2+}-induced SR Ca^{2+} release does not occur (Ikemoto et al., 1991; Ohkura et al., 1995). In our model, we propose that CSQ acts not only as a simple Ca^{2+} buffer, but also as a sensor of luminal SR Ca^{2+} load that exerts an effect on SRRC activatability.

Briefly, we propose that Ca^{2+} binding to fast activation sites on SRRCs promotes SRRC opening, the initial release of Ca^{2+} from the SR, and the dissociation of Ca^{2+} from CSQ. The dissociation of Ca^{2+} from CSQ is then assumed to be accompanied by a conformational change in the CSQ that not only modifies the Ca^{2+} binding characteristics of CSQ (Ikemoto et al., 1989; Gilchrist et al., 1992), but also is sensed by and modulates the inactivation characteristics of the SRRC (see Appendix B for a detailed description and rationale). This type of feedback accomplishes Ca^{2+} release termination in a single Ca^{2+} pool SR model in a system that exhibits gradedness and fractional Ca^{2+} release. This arm of the hypothetical control loop between SRRC and CSQ is perfectly consistent with the experimental observations that Ca^{2+}-dependent release of Ca^{2+} only occurs with a steep load dependence after a threshold level of Ca^{2+} in the SR is achieved (Gilchrist et al., 1992; Bassani et al., 1995) (for simulation, see Fig. 3 *B*). In the absence of some sort of communication between the SRRC and a luminal SR Ca^{2+} sensing element, it is intuitively difficult to reconcile these experimental data with a simple local Ca^{2+} depletion model for the termination of Ca^{2+} release.

As pointed out in the Results section, our simulated version of the graded response approximated the response observed by Fabiato (1985) but was not superimposable on it. There are several probable reasons for this apparent quantitative disparity. First, different response metrics were used in both experiments (tension versus $[Ca^{2+}]_c$), and it is well known that peak $[Ca^{2+}]_c$ is not linearly related to tension development (Backx et al., 1995). Second, in our simulation of the Fabiato experiment (Fabiato, 1985), we applied a bulk change in Ca^{2+} to a rat cardiocyte model, whereas in the actual experiment, canine myocardium was used. Third, in skinned fiber experiments (e.g., Fabiato, 1985), cellular Ca^{2+} buffers might be expected to have a smaller effect on the effectiveness of trigger Ca^{2+} to elicit SR Ca^{2+} release at the lower $[Ca^{2+}]$ when compared to whole cells (e.g., the model). This might explain the initial sigmoidal response at lower pCa values for our simulation compared to the linear response of the actual experiment (Fabiato, 1985). Nonetheless, all of the basic characteristics of a graded response were produced by our model.

SR Ca^{2+} leak versus uptake

As stated previously, the simulations depicting the consequences of the SR thermodynamic gradient are not particularly surprising when one considers the way in which the

model was constructed. However, the simulation experiments illustrated in Fig. 2 address several very fundamental concepts. There has been some dispute over whether the SR Ca^{2+} load is limited by SR Ca^{2+} uptake/back-flux (Shannon and Bers, 1997; Ginsburg et al., 1998; Shannon et al., 2000) or by the SR Ca^{2+} leak (O'Neill et al., 1999; Lukanyenko et al., 2000). In the context of our theory of control, the simple simulations depicted in Fig. 2 *A* underscore the idea that SR Ca^{2+} load is maintained below the thermodynamic limit and is, therefore, determined by the dynamic interaction of the thermodynamically limited SR Ca^{2+} uptake and the SR Ca^{2+} leak, and that a significant avenue of Ca^{2+} leak may be through open SRRCs. This latter idea is consistent with recent findings from Lukynanenko et al. (2000), suggesting that SR Ca^{2+} content is regulated by Ca^{2+} leak through SRRCs. In addition, there have been observations that in SR vesicles, Ca^{2+} load can only approach a thermodynamic maximum when SRRCs are blocked (Shannon and Bers, 1997), and in intact cardiocytes, SR Ca^{2+} load increases with SRRC blockade (O'Neill et al., 1999). Our model predicts that SR luminal Ca^{2+} limitations on SR uptake account for ~40% and SRRC leak for ~60% of the dynamic balance that determines SR Ca^{2+} content at quiescence.

In contrast, Shannon et al. (2000) recently developed mathematical descriptions of cellular Ca^{2+} fluxes in which SRRC leak was assumed to play a minor role in the determination of SR Ca^{2+} load, whereas primary control occurred via the regulation of forward and reverse Ca^{2+} fluxes through the SR Ca^{2+} pump. Key features in the development of the SR pump back-flux model of Shannon et al. (2000) are that the diastolic SRRC Ca^{2+} leak rate is very low (Bassani and Bers, 1995), SR Ca^{2+} load is primarily controlled by the concerted regulation of forward and backward Ca^{2+} fluxes through the SR Ca^{2+} pump, and that reverse flux (or back-flux) through the SR Ca^{2+} pump is linked to ATP production. The latter feature is intuitively very attractive because this mechanism of diastolic SR Ca^{2+} load control would be more favorable energetically than a scheme where Ca^{2+} is cycled through the SR via SRRCs. In comparison, in our model SR Ca^{2+} uptake rate is regulated by luminal Ca^{2+} in a manner similar to that proposed by Shannon et al. (2000), but back-flux per se is not represented. Our model predicts that diastolic SRRC leak is similar to that proposed by others (Wier et al., 1994) but is much greater than that estimated by Bassani and Bers (1995) and assumed for the back-flux scheme (Shannon et al., 2000). Two points are particularly relevant regarding this apparent leak discrepancy. First, our SR Ca^{2+} leak simulations (Fig. 2 *B*) indicate that the SRRC Ca^{2+} leak rate may be experimentally condition dependent, an idea previously acknowledged by Shannon et al. (2000) and one worth considering as a possible explanation for this discrepancy. Second, as pointed out by Shannon et al. (2000), the type of sarcoreticular Ca^{2+} cycling represented by our model would be expected to be less energetically economical than Ca^{2+} cycling via a back-flux mechanism, particularly in systems where the heart rate is slow and diastole is prolonged. In systems where heart rates are high (i.e., rat, ≥300 bpm) and in which diastolic resting states similar to those observed experimentally in isolated myocytes would never be achieved, the energetic consequences of back-flux might be of lesser importance. Nonetheless, this is clearly a concept that should not be overlooked.

The issue regarding the quantitative importance of SRRC Ca^{2+} leak and SR pump/back-flux activity in determining SR Ca^{2+} load is clearly one in need of closer scrutiny. Resolution of this issue is directly relevant to our model insofar as a key regulatory feature of the model that is central to its ability to handle a broad array of physiological predictions is a hypothetical, bidirectional interaction between SRRCs and CSQ. This interaction is directly and powerfully influenced by SR Ca^{2+} load.

The dependence of SR Ca^{2+} release on SR Ca^{2+} load

As discussed earlier, a central element of the current model that confers a properly scaled graded response on our system is the bidirectional communication between CSQ and SRRCs. This feature is also critical to the ability of the model to recapitulate the steep SR Ca^{2+} load dependence of SR Ca^{2+} release (Fig. 3 *B*). The data (simulated and experimental; Bassani et al., 1995) in Fig. 3 *B* are conceptually important for several reasons. First, in the context of our model, the CSQ:SRRC mechanism is critical in conferring a threshold for SR Ca^{2+} release that is strongly dependent on SR luminal Ca^{2+} content (discussed in detail in Appendix B). Second, the data in Fig. 3 *B* also illustrate the concept that SR Ca^{2+} content is limited by a dynamic balance between SR Ca^{2+} uptake and leak. Collectively, these mechanisms define the relatively narrow operating range of SR Ca^{2+} load in which the load is attainable and releasable. This behavior would not be possible if the SR acted as a simple Ca^{2+} pool.

Duration dependence of SR Ca^{2+} release varies with Ca^{2+} trigger and SR load

SR Ca^{2+} load and the Ca^{2+} trigger not only affect SR Ca^{2+} release directly (Fig. 3, *A* and *B*), but also indirectly by shifting the effect of Ca^{2+} trigger duration (Fig. 3 *C*). (Han et al., 1994; Isenberg and Han, 1994; Spencer and Berlin, 1995). The inclusion in the model of the CSQ:SRRC mechanism is crucial in providing the regulation of the SRRCs by Ca^{2+} on both sides of the SR membrane, which is necessary to reproduce these results. Overall, SR luminal Ca^{2+} feedback to the SRRCs and SR uptake is conceptually important from an integrative standpoint as a key connection in the interdependence of SR Ca^{2+} load, SR Ca^{2+} release, SR leak, SR uptake, $[Ca^{2+}]_c$, trigger size, and trigger duration (Figs. 2 and 3).

Time-dependent recovery of SR Ca^{2+} release

The current model was sufficient to reproduce a time-dependent recovery of the ability to release Ca^{2+} similar to that observed experimentally (Fig. 4). From our simulations, it appears that this was primarily related to SRRC refractoriness (with a minor effect due to SR Ca^{2+} reuptake). It has been proposed that there could be two additional factors affecting the recovery of the CICR response: 1) recovery of the L-type channels from inactivation and 2) diffusion of SR Ca^{2+} from an "uptake region" to a "release region" (for a review see Bers, 1993). Based on previous estimates, L-type Ca^{2+} channel recovery should only require ~300 ms (Mokelke et al., 1997), and intra-SR Ca^{2+} diffusion should take ~1 ms (Bers, 1993). In view of the fact that the experimentally observed (Cheng et al., 1996) and simulated half-times for recovery of SR Ca^{2+} release were >400 ms, these alternative processes appear to be too fast to be centrally related to the SR Ca^{2+} release recovery process at the pacing rates that were examined in both studies. We concede, however, that at faster pacing frequencies such as those that would be expected to occur physiologically in the rat (>300 bpm), at least one of these other processes might be expected to come into play.

There was one key difference between the model simulation and the time-dependent recovery of Ca^{2+} release experiment (Cheng et al., 1996). The model was of an isolated rat cardiac myocyte, whereas the actual experiment involved the observation of $[Ca^{2+}]$ changes in spaces in which Ca^{2+} sparks were observed in rat cardiocytes. The phenomenon of Ca^{2+} sparks is relevant to our model, although it was not specifically incorporated. Spark studies have shown that there are small individual cellular spaces ordered about the Z-lines within the cardiac myocytes. These individual spaces can undergo spontaneous SR Ca^{2+} release in a quiescent cell. If the SRRCs of the adjacent spaces are not in the refractory state, the Ca^{2+} spark can spread to these spaces, starting a wave (Cheng et al., 1996; Satoh et al., 1997). Where this theory applies to our model lies in the idea that with stimulation of the cell, many of these spaces in the cell may undergo CICR at once and become synchronized in their cycling through the refractory state. Our model represented the composite averaging of the fuzzy spaces undergoing CICR simultaneously, which may in turn represent a summation of the spark mechanisms in a whole-cell response.

Contraction frequency

The control features of the current model were adequate to reproduce a variety of fundamental pacing frequency-dependent characteristics, including rest potentiation, the negative "staircase" phenomenon, and extrasystolic potentiation. The negative staircase is a phenomenon that is rather unique to the myocardium of rats and other small rodents (Bers, 1993). In general, steady-state frequency-dependent alterations in contractile force are thought to be due to frequency-dependent alterations in the fractional release of Ca^{2+} from the SR and in the amount of releasable Ca^{2+} that is present in the SR. However, unlike myocardium from other species (Bers, 1993), several pieces of evidence suggest that the latter mechanism is of only modest to minor importance in rat myocardium (Stauffer et al., 1997; Bouchard and Bose, 1989; Bers, 1989). This is relevant to our model for several reasons. In our simulations the dominant response to steady-state increases in contraction frequency was a reduction in the fractional release of Ca^{2+} from the SR, whereas SR Ca^{2+} load was not significantly influenced (Fig. 6, *C* and *D*). The frequency-dependent effect on SR Ca^{2+} release was associated with the temporal characteristics with which SRRCs cycled through their functional states (Fig. 6, *E* and *F*), and this mechanism alone was sufficient to produce the negative staircase phenomenon. Insofar as SR Ca^{2+} load does not appear to be a dominant factor in the responsiveness of rat myocardium to pacing frequencies <2 Hz (Stauffer et al., 1997; Bouchard and Bose, 1989; Bers, 1989), it is reasonable to assume that changes in pacing frequency do not invoke large imbalances in cellular Ca^{2+} influx and efflux. However, it should be recognized that our simplified representation of sarcolemmal Ca^{2+} influx and efflux processes precludes the use of our model to rigorously examine the effects of pacing frequency on SR Ca^{2+} content. A more sophisticated representation of the sarcolemma would be required if this model were to be applied to systems in which the effect of pacing frequency on SR Ca^{2+} load are known to be substantial (i.e., guinea pig, rabbit).

Finally, an interesting and somewhat unexpected result of this study was the creation of cyclically variable (unstable) Ca^{2+} release states under conditions where cardiocyte Ca^{2+} overload was simulated. The unstable state had alternans-like characteristics that have been associated with a variety of pathological states, including cellular Ca^{2+} overload (Kihara and Morgan, 1991; Wohlfart, 1982). It has been proposed that the alternans condition is due to cyclic alterations in the refractory state of SRRC that occur secondary to alternating high and low fuzzy space $[Ca^{2+}]$ (Kihara and Morgan, 1991; Wohlfart, 1982). However, in our model, subtle loss of control in the bidirectional regulatory loop between SRRCs and SR luminal Ca^{2+} sensing elements appeared to be a major factor in altering SRRC refractoriness and SR Ca^{2+} releasability. This potential site of acute maladaptation is particularly interesting in view of the fact that the inclusion of the bidirectional SRRC-SR lumen regulatory loop was centrally important in the model's ability to recapitulate a broad array of normal, physiologically observable characteristics.

Context and limitations

It is readily recognized that the key elements of Ca^{2+} regulation represented in our model are intracellular processes that exist within a boundary about which key as-

sumptions must be made. This boundary limitation is unavoidable and inherent to all simulation models. In our model, the sarcolemma represents the boundary, or outer shell, about which we have made several simple regulatory assumptions, and within which the fundamental control elements of our model exist. Our outer shell assumptions were that 1) each contraction-relaxation cycle is initiated by a small, transient influx of Ca^{2+} into the cell via a fuzzy space, and 2) during a contraction steady state, cellular Ca^{2+} efflux varies as a function of changes in sarcoplasmic $[Ca^{2+}]$, and overall Ca^{2+} efflux must quantitatively approximate the magnitude of Ca^{2+} influx into the cell. With only several exceptions (Rice et al., 1999; Jafri et al., 1998), this is the type of approach that has been taken in the development and testing of most models of cardiocyte Ca^{2+} regulation to date (Wong et al., 1992; Tang and Othmer, 1994; Peskoff et al., 1992; Langer and Peskoff, 1996). Viewed in one way, this approach is a limitation because it clearly oversimplifies the complex sarcolemmal events that are known to be directly and/or indirectly involved in the regulation of transarcolemmal Ca^{2+} movement. On the other hand, it is relevant to note that in a model where sarcolemmal ion regulatory complexities were most comprehensively represented (Jafri et al., 1998), many of the most fundamental Ca^{2+} control mechanisms that were responsible for defining the size and shape of the cytosolic $[Ca^{2+}]$ transient were distal to events that occurred at the level of the sarcolemma. Moreover, that model was not sufficient to generate simulations of a graded response, whereas the current model (as well as others; Tang and Othmer, 1994; Glukhovsky et al., 1998) was. The differences in the abilities of the models to recapitulate this fundamental cellular response can be localized to differences in the theoretical representations of SR Ca^{2+} handling characteristics and not to differences in the representation of sarcolemmal Ca^{2+} handling. In summary, the most robust predictive capabilities of our model are inherent to regulatory processes that exist inside of a simplified sarcolemma or outer shell, and it is fully recognized that the inclusion of a more sophisticated representation of sarcolemmal Ca^{2+} influx and efflux processes would be expected to modulate the predictive capabilities of our model.

SUMMARY

Over the last decade, several models of cardiocyte Ca^{2+} regulation have been advanced, and each has made significant contributions to our understanding of the types of processes that are likely to be involved in the beat-to-beat regulation of sarcoplasmic $[Ca^{2+}]$. Unique features of the current model that significantly add to and conceptually extend earlier models of cardiocyte $[Ca^{2+}]$ regulation include 1) a quiescent steady-state (starting point) condition that was self-defined by the same model control elements that governed dynamic model responses; 2) bidirectional regulatory influences between the SRRCS and SR luminal $[Ca^{2+}]$ that are mediated by CSQ; and 3) a thermodynamic limit for the $[Ca^{2+}]$ gradient that exists across the SR membrane. The current macroscopic model of cardiocyte Ca^{2+} regulation is sufficient to predict a wide variety of fundamental physiological responses, and to our knowledge, no other previously published model can accommodate a comparable predictive breadth. The theory of cellular Ca^{2+} control advanced by our model shows promise in bridging the gap between our understanding of isolated cell processes and how those processes can be integrated to produce a whole-cell response. Specifically, the model as constructed readily lends itself to further tests and modifications. Viewed in this way, current and future model predictions should prove useful in the design and analysis of experiments that seek to determine how a variety of individual cellular processes might be integrated to elicit specific normal or pathological cellular responses.

APPENDIX A: THE MODEL EQUATIONS

This mathematical model represented Ca^{2+} movement across the sarcolemma and between three intracellular compartments capable of buffering Ca^{2+} (see Fig. 1). The model comprised six ordinary differential equations. Three differential equations described the rates of change of free Ca^{2+} concentrations in three intracellular compartments representing the cytosol, the SR, and the fuzzy space. The Ca^{2+} buffers of the cytosol and the fuzzy space were represented as instantaneous within the differential equations for those compartments. The Ca^{2+} buffering of the SR was represented by a separate differential equation. Finally, two differential equations described the kinetics of the SRRC, which governed the release rate constant of the SRRC. The mathematical representations of the movement mechanisms, the influence of Ca^{2+} buffering, and the resultant differential equations are presented below.

Ca^{2+} movement mechanisms

Ca^{2+} influx across the sarcolemma

The rate of extracellular Ca^{2+} entry into the fuzzy space was represented by a first-order linear diffusion process:

$$k_1([Ca^{2+}]_e - [Ca^{2+}]_f), \quad (1)$$

where k_1 is the rate constant analogous to the collective conductance of L-type channels, $[Ca^{2+}]_e$ is the free Ca^{2+} concentration in the extracellular space, and $[Ca^{2+}]_f$ is the free Ca^{2+} concentration in the fuzzy space. Ca^{2+} influx across the sarcolemma was initiated by setting k_1 equal to a specified rate constant value for a 0.02-s interval (Langer and Peskoff, 1996), thereby simulating the action potential-stimulated opening of the L-type channels and reversed Na^+-Ca^{2+} exchange. During the time remaining until the next simulated stimulation, the k_1 value was set to represent sarcolemma leak, which was estimated in the calculation of the steady-state conditions at quiescence, described in Materials and Methods. Note that with the sizes of the SR Ca^{2+} load and the L-type Ca^{2+} trigger of the model, the effect of Ca^{2+} trigger duration (>5 ms) is limited to the impact on the overall equilibrium achieved between cellular Ca^{2+} influx and efflux processes (see Fig. 3 *C* and related Discussion).

Ca^{2+} movement through SRRC

Ca^{2+} movement through the SRRC was modeled to be dependent on the Ca^{2+}-bound state of the SRRC and was representative of calcium-induced

calcium release. The free Ca^{2+} in the fuzzy space was modeled to bind with the SRRCs, which have been proposed to contain two different types of binding sites, fast and slow (Fabiato, 1985). The binding of free Ca^{2+} to the SRRC was modeled with the following kinetics:

$$Ca^{2+} + S_i \leftrightarrow Ca^{2+}S_i + Ca^{2+} \leftarrow \cdots \rightarrow (Ca^{2+})_n S_i, \quad (2)$$

where S_i is the ith binding site, such that S_1 is the fast binding site (activating) and S_2 is the slow binding site (inactivating), and n is the minimum number of Ca^{2+} ions that bind to each type of site on a single channel.

Activation of a single SR Ca^{2+} release channel was assumed to involve two binding steps, each encompassing the binding of a Ca^{2+} ion to an activating site with a high level of cooperativity (Fabiato, 1985; Sham et al., 1995). The assumption of strong cooperativity led to the following further assumptions for the two-step binding reaction: 1) the first Ca^{2+} binding was the rate-limiting step, 2) the first Ca^{2+}-binding step enhanced the second Ca^{2+}-binding step to the same degree in both directions (for binding and dissociation from the site), 3) the second binding step would be at equilibrium, and 4) $[(Ca^{2+})_2S_1] \gg [Ca^{2+}S_1]$. These assumptions were used to develop the following equation, which described the rate of change in the concentration of a Ca^{2+}-bound activating site:

$$\frac{d[(Ca^{2+})_2 S_1]}{dt} = k_{on,1}[Ca^{2+}]_f[S_1] - \left(\frac{k_{off,1}^2}{k_{on,1}[Ca^{2+}]}\right)_f[(Ca^{2+})_2S_1], \quad (3a)$$

where $[(Ca^{2+})_2S_1]$ is the concentration of Ca^{2+} bound to the activating site, $[S_1]$ is the free concentration of the activating binding site, i.e., $[S_1]_{total} - [(Ca^{2+})_2S_1]$, $k_{on,1}$ is the binding rate constant, and $k_{off,1}$ is the dissociation rate constant.

Inactivation of a single SR Ca^{2+} release channel was assumed to follow first-order kinetics in each reactant with the binding of one Ca^{2+} ion to a single inactivating site (Fabiato, 1985):

$$\frac{d[Ca^{2+}S_2]}{dt} = k_{on,2}[Ca^{2+}]_f[S_2] - k_{off,2}[Ca^{2+}S_2], \quad (3b)$$

where $[Ca^{2+}S_2]$ is the concentration of Ca^{2+} bound to the inactivating site, $[S_2]$ is the free concentration of the inactivating binding site, i.e., $[S_2]_{total} - [Ca^{2+}S_2]$, $k_{on,2}$ is the binding rate constant, and $k_{off,2}$ is the dissociation rate constant.

The fractional concentrations of bound sites, defined as $cas_i = [(Ca^{2+})_nS_i]/[S_i]_{total}$, were governed by the equations

$$\frac{dcas_1}{dt} = k_{on,1}[Ca^{2+}]_f(1 - cas_1) - \frac{k_{off,1}^2}{k_{on,1}[Ca^{2+}]_f}cas_1, \quad (4a)$$

$$\frac{dcas_2}{dt} = k_{on,2}[Ca^{2+}]_f(1 - cas_2) - k_{off,2}cas_2. \quad (4b)$$

The functional state of the SRRC depended on the combination of the calcium-bound states of the fast and slow binding sites (Fabiato, 1985; Coronado et al., 1994). In this model, the four possible states were as follows: 1) activatable: no Ca^{2+} bound, 2) open: Ca^{2+} bound to fast site only, 3) closed: Ca^{2+} bound to both sites, and 4) refractory: Ca^{2+} bound to slow site only. The fractions of SRRC that were in each of the four functional states were determined as follows:

$$\text{SRRC fraction activatable:} \quad r_a = (1 - cas_1)(1 - cas_2) \quad (5a)$$

$$\text{SRRC fraction open:} \quad r_o = cas_1(1 - cas_2) \quad (5b)$$

$$\text{SRRC fraction refractory:} \quad r_r = cas_2(1 - cas_1) \quad (5c)$$

$$\text{SRRC fraction closed:} \quad r_c = cas_1 \cdot cas_2 \quad (5d)$$

Finally, movement of Ca^{2+} through the SRRC was modeled to be linearly proportional to the concentration difference and the fraction of open SRRC (r_o):

$$k_s \cdot r_o([Ca^{2+}]_s - [Ca^{2+}]_f), \quad (6)$$

where k_s is the rate constant analogous to the collective conductance of SRRC, and $[Ca^{2+}]_s$ is the free Ca^{2+} concentration in the SR. Equations 6 and 4 represent the regulation of CICR. Leak from the SR also occurred through the SRRC, because there was always a fraction of SRRC in the open state due to the presence of a baseline level of Ca^{2+} in the fuzzy space.

Ca^{2+} efflux across the sarcolemma by Na^+-Ca^{2+} exchange

Transport of Ca^{2+} into the extracellular space from the fuzzy space by the Na^+-Ca^{2+} exchanger was modeled to follow Michaelis-Menten kinetics:

$$\frac{V_{max,NaCaX}[Ca^{2+}]_f}{K_{m,NaCaX} + [Ca^{2+}]_f}, \quad (7)$$

where $V_{max,NaCaX}$ is the maximum rate of Ca^{2+} removal, and $K_{m,NaCaX}$ is the dissociation constant (Philipson and Nishimoto, 1981; Reeves and Sutko, 1983; Tibbits et al., 1989). Ca^{2+} influx across the sarcolemma was initiated using Eq. 1 to simulate the action potential-stimulated opening of the L-type channels and reversed Na^+-Ca^{2+} exchange for a 0.02-s interval. Therefore $V_{max,NaCaX}$ of Eq. 7 was set to 0 during the 0.02-s opening interval. It should be reiterated that one of the key assumptions that we made in our use of a simplified representation of cellular Ca^{2+} influx and efflux processes was that over time, both processes were assumed to be reasonably balanced during any steady state to avoid large changes in cellular Ca^{2+} load over short periods of time. In our model, this was true at pacing frequencies below 2 Hz. However, with the simulation of pacing rates at or above 2 Hz, the model as constructed demonstrated a tendency to overload the cytosol with Ca^{2+} over time. This imbalance between Ca^{2+} influx and efflux could be rectified with a minor adjustment of the sodium-calcium exchange dissociation constant (25% reduction). Alternatively, this adjustment could have been accomplished via a small reduction in the duration of the Ca^{2+} trigger current, consistent with the known effect of pacing frequency on cardiac action potential duration. Neither adjustment method would have had a noticeable impact on the function of our model in any of the simulations.

Ca^{2+} movement between the fuzzy space and cytosol

The Ca^{2+} movement between the fuzzy space and the cytosol was modeled to be linearly proportional to the concentration difference,

$$k_f([Ca^{2+}]_f - [Ca^{2+}]_c), \quad (8)$$

where k_f is the diffusion rate constant between the fuzzy space and the cytosol.

Ca^{2+} uptake by SR Ca^{2+}-ATPase

The rate of Ca^{2+} uptake by the SR was modeled to follow second-order reversible Michaelis-Menten kinetics:

$$\frac{V_{max,s}([Ca^{2+}]_c^2 - [Ca^{2+}]_s^2/7000^2)}{(K_{m,s}^2 + [Ca^{2+}]_c^2 + [Ca^{2+}]_s^2/7000^2)}, \quad (9)$$

where V_{max} is the maximum rate of uptake by the SR, and K_m is the dissociation constant. Equation 9 was based on a form of an Henri/Michaelis-Menten sequence, which accounts for feedback from the product ($[Ca^{2+}]_s$) of the reaction (SR uptake). Equation 9 was designed to account for the thermodynamically limited gradient of 7000 that the SR Ca^{2+}-ATPase can produce between the cytosol and the SR (Shannon and Bers, 1997). Note that in typical studies of SR uptake, oxaloacetate anion is used to precipitate the Ca^{2+} in the SR, resulting in free $[Ca^{2+}]_s \approx 0$, which would reduce Eq. 9 to the form cited in many studies (Stienen et al., 1995; Mattiazzi et al., 1994; Bers and Berlin, 1995):

$$\frac{V_{max,s}[Ca^{2+}]_c^2}{(K_{m,s}^2 + [Ca^{2+}]_c^2)}. \quad (10)$$

Ca^{2+} buffering

Ca^{2+} buffering in the cytosol and the fuzzy space

The cytosol and the fuzzy space were assumed to contain Ca^{2+} buffers with which free Ca^{2+} would instantaneously equilibrate. (Note that for the cytosol, parameter values were used to represent the key fast buffers that would be in phase with the $[Ca^{2+}]_c$ transient (Berlin et al., 1994), as described in Appendix B.) Following much of the development presented by Bers and Berlin (1995), the total Ca^{2+} concentration in any one compartment was the sum of free and bound Ca^{2+} concentrations:

$$[Ca]_{Total} = [Ca]_{Free} + \frac{B_{max}}{[1 + (K_b/[Ca]_{Free})^n]}, \quad (11)$$

where B_{max} is the maximum free buffer concentration, K_b is the buffer dissociation constant, and n is the Hill coefficient. Changes in $[Ca^{2+}]_{Free}$ relative to changes in $[Ca^{2+}]_{Total}$ were determined by the chain rule:

$$\frac{d[Ca^{2+}]_{Total}}{dt} = \frac{d[Ca^{2+}]_{Free}}{dt}\frac{d[Ca^{2+}]_{Total}}{d[Ca^{2+}]_{Free}}; \quad (12)$$

therefore,

$$\frac{d[Ca^{2+}]_{Total}}{dt} = \frac{d[Ca^{2+}]_{Free}}{dt}\left\{\frac{n \cdot B_{max} \cdot [Ca^{2+}]^{n-1} \cdot K_b^n}{([Ca^{2+}]^n + K_b^n)^2} + 1\right\}. \quad (13)$$

Those differential equations meant to represent the rate of change of the free Ca^{2+} concentrations will be equal to the rate of change in total $[Ca^{2+}]$ divided by a denominator, which is the bracketed term in the Eq. 13 with the Hill coefficient set equal to one.

Ca^{2+} buffering in the SR

With bidirectional feedback between the SRRC and CSQ, the Ca^{2+} buffering of the SR could not be effectively modeled to be instantaneous, but was instead represented by the following differential equation:

$$\frac{d[Ca^{2+}CSQ]}{dt} = k_{on,s}[Ca^{2+}]_s(B_{max,s} - [Ca^{2+}CSQ]) - k_{off,s}[Ca^{2+}CSQ], \quad (14)$$

where $[Ca^{2+}CSQ]$ is the concentration of Ca^{2+} bound to the CSQ, $k_{on,s}$ is the binding rate constant, $k_{off,s}$ is the dissociation rate constant, and $B_{max,s}$ is the maximum free buffer concentration.

The bidirectional mechanism was modeled as feedback-induced shifts of the Ca^{2+} binding curves of CSQ and SRRCs. A detailed description of the evidence and the implementation of these internally controlled shifts are provided in Appendix B.

The compartmental differential equations

The rates of change of free Ca^{2+} concentrations in each of the three intracellular compartments were represented by three differential equations. These equations represented the rates of change of total Ca^{2+} concentrations due to Ca^{2+} movement into and out of each compartment. Furthermore, the equations for the cytosol and the fuzzy space were divided by the bracketed term of Eq. 13 to account for free Ca^{2+} equilibration with the respective buffers.

The parameters represented quantities in reference to the entire cell water. Therefore the appropriate volume fractions were divided through to convert to compartmental changes; this is reflected in the differential equations described below.

Fuzzy space

The following Ca^{2+} processes were considered in representing free Ca^{2+} concentration in the fuzzy space: L-type channels, leak from the extracellular space, Ca^{2+} binding to the SRRC sites incorporating concentration of the sites (R_t), CICR from the SR, diffusion to the cytosol, and Na^+-Ca^{2+} exchange. Two types of sarcolemma Ca^{2+} buffering sites were represented as described by Langer and Peskoff (1996) and using the bracketed part of Eq. 13. In addition, the influence of Ca^{2+} bound to the SRRC was included:

$$\frac{d[Ca^{2+}]_f}{dt} = \frac{\left\{\begin{array}{r} k_s \cdot r_o([Ca^{2+}]_s - [Ca^{2+}]_f) - (dcas_1/dt + dcas_2/dt)R_t \\ - k_f([Ca^{2+}]_f - [Ca^{2+}]_c) + k_l([Ca^{2+}]_e - [Ca^{2+}]_f \\ - V_{max,NaCaX}[Ca^{2+}]_f/(K_{m,NaCaX} + [Ca^{2+}]_f) \end{array}\right\}}{\frac{B_{max,f1} \cdot K_{b,f1}}{([Ca^{2+}]_{f1} + K_{b,f1})^2} + \frac{B_{max,f2} \cdot K_{b,f2}}{([Ca^{2+}]_{f2} + K_{b,f2})^2} + V_f}. \quad (15)$$

Cytosol

The following Ca^{2+} movement processes were considered in representing free Ca^{2+} concentration in the cytosol: SR Ca^{2+}-ATPase and diffusion from the fuzzy space. All of the fast passive buffers of the cytosol were represented as one buffer as described by a fit to a binding curve presented by Bers and Berlin (1995), with the parameter values from Berlin et al. (1994). In experiments where a dye indicator such as fura-2 was used, the resulting buffering was included as represented in the bracketed part of Eq. 13:

$$\frac{d[Ca^{2+}]_c}{dt} = \frac{k_f([Ca^{2+}]_f - [Ca^{2+}]_c) - \frac{V_{max,s}([Ca^{2+}]_c - [Ca^{2+}]_s^2/7000^2)}{(K_{m,s}^2 + [Ca^{2+}]_c^2 + [Ca^{2+}]_s^2/7000^2)}}{\frac{B_{max,c} \cdot K_{b,c}}{([Ca^{2+}]_c + K_{b,c})^2} + \frac{[dye]_c \cdot K_{b,dye}}{([Ca^{2+}]_c + K_{b,dye})^2} + V_c}. \quad (16)$$

Sarcoplasmic reticulum

The following Ca^{2+} movement processes were considered in representing free Ca^{2+} concentration in the SR: SR Ca^{2+}-ATPase and CICR from the SR. The buffering was represented as described in Eq. 14:

$$\frac{d[Ca^{2+}]_s}{dt} = \left(\frac{V_{max,s}([Ca^{2+}]_c^2 - [Ca^{2+}]_s^2/7000^2)}{(K_{m,s}^2 + [Ca^{2+}]_c^2 + [Ca^{2+}]_s^2/7000^2)} - k_s \cdot r_o([Ca^{2+}]_s - [Ca^{2+}]_f) \right) \Big/ V_s - \frac{d[Ca^{2+}CSQ]}{dt}. \quad (17)$$

APPENDIX B: THE MODEL PARAMETERS

To represent the accessible water volume of the cell that was not mitochondria and not sarcomeric protein, the following value was used: 0.5 L cell water/1 L cell total volume (refer to Berlin et al., 1994; Page et al., 1971; Page, 1978; Sipido and Wier, 1991). Each of the model parameters has been derived to represent the changes relative to accessible cell water. Therefore all of the molarity values are in mol/L of cell water (unless otherwise noted). Values relative to the cellular compartments were converted within the model differential equations by adjustments based on volume fractions. It should also be noted that the model output values were compared to experimentally determined values (Table 3), which were converted to represent mol/L of cell water, as defined in this study.

SRRC concentration

The model value for the SRRC concentration was $R_t = 1.5 \times 10^{-7}$ M. This value was derived from the estimated value of 1.6×10^6 SRRCs per cell (Bassani and Bers, 1995), which had been derived from a measured value representing the concentration of ryanodine receptor sites in the whole cell, 833 fmol/mg protein (Bers and Stiffel, 1993). The model value was based on a total cell volume of 36.8 pl (Delbridge et al., 1997) with 0.5 L cell water/L cell total volume (see above).

The model value for SRRC concentration could also be determined by a series of calculations similar to those used in Langer's model of the diadic cleft (Langer and Peskoff, 1996). First, the number of individual sarcomeric units (domains bounded by SR) per cell was estimated as follows. Using a total cell volume of 36.8 pl (Delbridge et al., 1997), an individual sarcomeric volume of 1.37 μm^3 (Langer and Peskoff, 1996), and a fraction of cell volume that is sarcomeric of 0.6 (Legato, 1979), it was estimated that there are $\sim 1.6 \times 10^4$ individual sarcomeric units (bound by SR and Z lines) per cell. It was assumed that there is one fuzzy space (or junction or diadic cleft) per individual sarcomeric unit, and that each fuzzy space contains a set of 100 SRRCs, following predictions from Wibo et al. (1991). It followed that there are 1.6×10^6 SRRCs per cell, which converted to 1.5×10^{-7} M (in convincing agreement with the above value of 1.5×10^{-7} M, which was based on the concentration of the ryanodine-binding sites). The agreement of the measured and calculated R_t values provided support for the assumptions and estimates necessary for the above calculations (e.g., the number of fuzzy spaces). These assumptions and estimates were useful for some of the further parameter calculations.

Volume fraction of the fuzzy space

The volume fraction of the fuzzy space, $V_f = 0.0013$ (fuzzy space volume/cell water volume), was calculated using the above estimate of 1.6×10^4 fuzzy spaces per cell. The calculation was based on the estimate by which individual fuzzy spaces were represented, with right cylinder dimensions of radius 200 nm (Radermacher et al., 1994) and height 12 nm (Langer and Peskoff, 1996), from a probable range of 10–20 nm (Sham et al., 1995). Additional values used for this calculation were 0.5 L cell water/L cell total volume and a total cell volume equal to 36.8 pl (Delbridge et al., 1997). It is important to note that the model V_f (0.0013) is in agreement with a range from Cannell et al. (1994), who estimated that the fuzzy space should be <0.0020 as a fraction of the cytosol (which converts to <0.0019 as a fraction of cell water).

Volume fraction of the SR

The volume fraction of the SR, $V_s = 0.07$ (SR volume/cell water volume), was taken from a value reported by Page (1978), 0.035 (SR volume/cell total volume), which was converted to represent the fraction of the cell water volume.

Volume fraction of the cytosol

The volume fraction of the cytosol, $V_c = 0.9287$ (cytosol volume/cell water volume), was calculated as $1 - V_f - V_s$.

Dissociation constants for the two sites of the SRRC

The dissociation constant for the fast binding site of the SRRC, $K_1 = k_{off1}/k_{on1} = 7.0 \times 10^{-7}$ M, and the dissociation constant for the slow binding site of the SRRC, $K_2 = k_{off2}/k_{on2} = 3.0 \times 10^{-7}$ M, were estimated to be within a range of values, 3.0×10^{-7} to 7.0×10^{-7} M, based on observations and predictions by Sham et al. (1995). In accordance with predictions by Fabiato (1985), the fast binding site was represented as having a low Ca^{2+} binding affinity, using the value at the high end of the range. The slow binding site was represented as having a high Ca^{2+} binding affinity, using the value from the low end of the range.

Binding rates for the two sites of the SRRC

The binding rates for the fast and slow binding sites of the SRRC, $k_{on,1} = 2.0 \times 10^9$ $(M \cdot s)^{-1}$ and $k_{on,2} = 1.3 \times 10^7$ $(M \cdot s)^{-1}$, were estimated to be within a range of the rates of binding of ions to proteins, 1.0×10^6 to 3.0×10^9 $(M \cdot s)^{-1}$, as estimated by Moore and Stull (1984) and as predicted using the Arrhenius expression in describing a diffusion-controlled reaction. For the Arrhenius expression, an encounter distance of 5.0×10^{-8} cm was assumed, and a diffusion coefficient of 7.9×10^{-7} cm^2/s (Marcus, 1997) was used to represent the most unobstructed access possible between the Ca^{2+} influx and the SRRC. Note that the upper limit of 3.0×10^9 $(M \cdot s)^{-1}$ would be somewhat larger if one represented the following: 1) a possible presence of electrostatic forces between the Ca^{2+} ions and the SRRC binding sites, and 2) a larger encounter distance due to the apparent size of the channel protein.

The model values were chosen for each site to represent the difference in binding rates as predicted by Fabiato (1985), such that the rate constant of Ca^{2+} binding to the inactivating site was lower than that to the activating site. A value of 1.3×10^7 $(M \cdot s)^{-1}$ is typical for an ion binding to a protein (Moore and Stull, 1984). A value of 2.0×10^9 $(M \cdot s)^{-1}$ would imply that the activating site binding reaction operates near the diffusion limit.

Hill coefficients for the two sites of the SRRC

The Hill coefficients represented the minimum number of Ca^{2+} ions that bind to the fast (activating) and slow (inactivating) binding sites for each SR Ca^{2+} release channel. In this model, there was the potential for two Ca^{2+} ions binding to the fast site(s) on each SR Ca^{2+} release channel ($n_1 = 2$) and one Ca^{2+} ion binding to the slow site on each SR Ca^{2+} release channel ($n_2 = 1$). There are a number of studies that support these

assumptions. For instance, Fabiato (1985) suggested that inactivation was caused by a first-order reaction of one Ca^{2+} ion binding to a single site (i.e., $n_2 = 1$). In addition, Fabiato speculated that the activation could represent a binding of more than one Ca^{2+} (i.e., $n_1 > 1$). In further support of $n_1 = 2$, Sham et al. (1995) determined a Hill slope of 2.1 for the activation of SR Ca^{2+} release, and Santana et al. (1996) observed that the probability of activation of a SR release unit depends on the square of the local $[Ca^{2+}]$.

SRRC Ca^{2+} release rate constant

The SRRC release rate constant (k_s) used in this model was 9 s^{-1}, representing the ease of movement of Ca^{2+} through the entire set of a cell's SRRCs. This value fell within the range of values measured and reviewed by Kim et al. (1983), from 2 to 139 s^{-1}, and within the range measured by Donoso et al. (1995), from 2 to 12 s^{-1}.

There were model results (Table 3) that further supported the use of $k_s = 9$ s^{-1}. The model-simulated value for the SR Ca^{2+} release rate was within the expected value. The model-simulated SR Ca^{2+} release flux integral was within a range of estimated and measured values. In addition, the fractional SR Ca^{2+} release was within the expected range.

L-type channel rate constant

The net L-type channel rate constant (k_l) was 0.2 s^{-1}, representing the ease of movement of Ca^{2+} through a collection of a cell's L-type channels for a set period of opening, with the probability of being open included within the rate constant value. This L-type rate constant value was approximately an order of magnitude less than the SRRC rate constant multiplied by the fraction of open SRRC, in agreement with results from Bers (1993).

There were some model results (Table 3) that supported the use of this value for the L-type rate constant. First, the model-simulated Ca^{2+} influx (integral) was within the expected range from the literature. In addition, the simulated Ca^{2+} influx was very close to the expected range.

Na^+-Ca^{2+} exchange

The maximum rate of Na^+-Ca^{2+} exchange, $V_{max,Na/CaX} = 1.2 \times 10^{-3}$ M/s, was converted directly from a measured value, 3.2 nmol/mg protein · s (Tibbits et al., 1989), using the values of ~110 mg protein/g wet weight (Tibbits et al., 1989), 0.57 ml cell volume/g wet weight (Page, 1978), and 0.5 L cell water/L cell total volume (from above). The Michaelis constant of the Na^+-Ca^{2+} exchange, $K_{m,Na/CaX} = 3.6 \times 10^{-5}$ M, was taken directly from a value determined by Tibbits et al. (1989), 3.6×10^{-5} M. The range for $K_{m,Na/CaX}$ has been observed to be 1.0×10^{-6} to 2.0×10^{-4} M (Tibbits et al., 1989; Sham et al., 1995; Philipson and Nishimoto, 1981; Reeves and Sutko, 1983; Hilgemann et al., 1992). The Hill coefficient, $n = 1$, was used as derived by Tibbits et al. (1989).

SR uptake

The maximum uptake rate of SR Ca^{2+}-ATPase, $V_{max,s} = 5.25 \times 10^{-4}$ M/s, was obtained from a range of values, 3.6×10^{-4} to 6.3×10^{-4} M/s (Bers, 1993; Stienen et al., 1995). The dissociation constant of the SR Ca^{2+}-ATPase, $K_{m,s} = 2.5 \times 10^{-7}$ M, was taken directly from a range of values, 2×10^{-7} to 8.3×10^{-7} M/s (Bers, 1993; Stienen et al., 1995; Mattiazzi et al., 1994; Bers and Berlin, 1995). The Hill coefficient for these studies was approximately $n = 2$, which was used in the model.

Diffusion constant

The diffusion constant, $k_f = 2500$ s^{-1}, described the ease of movement of Ca^{2+} between the fuzzy space and the cytosol. With a few assumptions, this value can be estimated using an equation reported by Chen et al. (1997) for flux through a channel described as a unimolecular reaction, where

$$k_f = (D_j/d^2) \cdot \text{Prob}\{\text{cytosol}|\text{fuzzy}\},$$

D_j is the two-dimensional diffusion coefficient, d is the length of the channel, and Prob{cytosol|fuzzy} is the conditional probability that a particle (Ca^{2+}) that is given to be in the fuzzy space will move to the cytosol.

This channel equation was applied to the fuzzy space based on the concept that the SR cisternal membrane may be in such close physical proximity to the sarcolemma that the region bound by these membranes can be considered to contain localized interactions typical of an enclosed compartment (Sham et al., 1995). Given the close physical proximity of the membranes, there should be a limited opening through which the Ca^{2+} could pass. The distance between the SR and SL membranes has been estimated to be 12 nm, and the space between them has been modeled as a right cylinder with a radius of 200 nm (Langer and Peskoff, 1996). With this in mind, the area of the outer surface of the side of the cylinder would represent the opening through which the Ca^{2+} would move. The modeled radius of 200 nm was used to estimate a relative length for use as d in the above equation.

In the literature, there are values for two-dimensional diffusion constants (D_j), which quantify the restricted and free movement of Ca^{2+} in aqueous solution, $\sim 7 \times 10^{-7}$ and 7.9×10^{-6} cm^2/s, respectively (Tillotson and Nasi, 1985; Marcus, 1997); for a review see Langer and Peskoff (1996). Prob{cytosol|fuzzy} was estimated based on the volume fractions of each compartment (~Prob(cytosol) = $V_c/(V_c + V_f)$).

There was a range for the estimated k_f based on the range for the diffusion coefficients and using the above equation, resulting in $k_f \approx 1.7 \times 10^3$ to 2.0×10^4 s^{-1}. For movement from the cytosol to the fuzzy space, volume fraction adjustments were used to approximate the estimate by using Prob{fuzzy|cytosol} (~Prob(fuzzy) = $V_f/(V_f + V_c)$) instead of Prob{cytosol|fuzzy}.

Extracellular Ca^{2+} concentration

The value for the extracellular Ca^{2+} concentration, $[Ca^{2+}]_e$, was 0.002 M, which is the level in the normal Tyrode's solutions typically used experimentally to bathe isolated cardiac myocytes.

Ca^{2+} buffering

All of the buffering parameters were taken directly from published values.

For purposes of simplification, instantaneous buffering was derived for the cytosol based on a study from Bers and Berlin (1995), in which a single binding curve was determined for the various Ca^{2+} binding sites of the cytosol. With the use of instantaneous buffering in the model, only key fast buffers were represented as those being in phase with the $[Ca^{2+}]_c$ transient (as opposed to equilibrium buffering). The maximum free buffer concentration of the cytosol, $B_{max,c} = 1.2 \times 10^{-4}$ M, and the buffer dissociation constant of the cytosol, $K_{b,c} = 9.6 \times 10^{-7}$ M, were from a study of Berlin et al. (1994), which appeared to have represented the fast buffers. For $B_{max,c}$, the range of estimated values from Berlin et al. (1994) was considered (8.6×10^{-4} to 2.0×10^{-4} M). The $B_{max,c}$ range was adjusted to account for the buffering already represented in the fuzzy space. In addition, the $B_{max,c}$ range was adjusted to account for nonprotein cell water. The cytosolic Ca^{2+} buffering has been observed to have an effect on the removal of Ca^{2+} (Bers and Berlin, 1995). The modeling of fast cytosolic buffering was therefore supported by the successful replication of active $[Ca^{2+}]_c$ clearance dynamics results (Table 3). Providing further support, the percentage of cytosolic Ca^{2+} free versus bound and the buffer power both corresponded to literature values (Table 3).

The model has the option of representing dye indicators, if relevant to the experiment to be simulated. The model value for the dye concentration in the cytosol depended on the experimental protocol and assumptions. The dissociation constant of the fura-2 was $K_{b,fura} = 2.0 \times 10^{-7}$ M, which was within the determined range of 1.0×10^{-7} to 3.0×10^{-7} M (Grynkiewicz et al., 1985; VanHardeveld et al., 1995). The dissociation constant for fluo-3 was 1.13×10^{-6} M (Smith et al., 1998).

The fuzzy space buffering was modeled to represent the observation of two different binding sites by Langer and Peskoff (1996), with the constants as follows: site 1: $B_{max,f1} = 2.0 \times 10^{-4}$ M (from 2.3×10^{-19} moles per fuzzy space) and $K_{b,f1} = 1.1 \times 10^{-3}$ M; and site 2: $B_{max,f2} = 1.7 \times 10^{-5}$ M (from 1.9×10^{-20} moles per fuzzy space) and $K_{b,f2} = 1.3 \times 10^{-5}$ M. The B_{max} values were converted to represent concentration in accessible cell water, using a value for the cell volume of 36.8 pl (Delbridge et al., 1997) and estimated values of $\sim 1.6 \times 10^4$ fuzzy spaces per cell and 0.5 L cell water/L cell total volume (from above).

The maximum free buffer concentration of the SR, $B_{max,s} = 0.008$ mol/L SR water, was from a range of values, 0.005–0.014 mol/L SR water (Bers, 1993; Shannon and Bers, 1997). The buffer dissociation constant of the SR, $K_{b,s} = 0.000638$ M, was taken directly from a value of Shannon and Bers (1997), 0.000638 M. The buffer on-rate constant, $k_{on,s} = 8772$ $M^{-1}s^{-1}$, was obtained directly from a value determined by Donoso et al. (1995), 8772 $M^{-1}s^{-1}$.

SRRC-CSQ bidirectional feedback

A very important innovation in this model was the inclusion of bidirectional interplay between the SRRC and CSQ, which was based on a series of published observations of striated muscle. It has been generally accepted that CSQ plays two roles: the binding of Ca^{2+} and the modulation of SR Ca^{2+} release (Donoso et al., 1995; Gilchrist et al., 1992; Gyorke and Gyorke, 1998; Hidalgo et al., 1996; Ikemoto et al., 1989,

First to be addressed is the possibility of feedback from the SRRC to CSQ, based on observations of an apparent triggered release of Ca^{2+} from CSQ (Ikemoto et al., 1991). It was shown that a trigger-induced rise in free [Ca^{2+}] in SR vesicles occurred immediately before SR Ca^{2+} release. In addition, the release of Ca^{2+} was triggered from CSQ that was bound to isolated SR junctional face membrane. Furthermore, CSQ not bound to SR junctional face membrane would not release Ca^{2+}. Without CSQ, the isolated SR junctional face membrane would also not release Ca^{2+} (also shown by Okhura et al., 1995). Reconstituted CSQ and SR junctional face membrane regained the ability to release Ca^{2+}. Ikemoto et al. (1991) proposed that this release of Ca^{2+} from the CSQ was induced by the transmission of the SR Ca^{2+} release trigger signal to the CSQ. Gilchrist et al. (1992) presented further evidence that the conformational states of the SRRC and the CSQ are coupled, which led to the suggestion that the affinity of CSQ for Ca^{2+} would be dependent on the state of the SRRC.

Our focus changes here to feedback from CSQ to the SRRC. It has been shown in a number of studies that SR lumen Ca^{2+} has an effect on 1) the probability of SRRC opening (Gyorke and Gyorke, 1998; Lukyanenko et al., 1996; Sitsapesan and Williams, 1997), 2) the rate constant of SR Ca^{2+} release (Ikemoto et al., 1989; Donoso et al., 1995), and 3) fractional SR Ca^{2+} release (Bassani et al., 1995). It is interesting to note that CSQ conformation and CSQ-Ca^{2+} binding (Hidalgo et al., 1996), SRRC probability of opening, and rate constant of Ca^{2+} release all respond to a similar luminal [Ca^{2+}] range with a similar sigmoidal response (this sigmoidal response can also be implied from the fractional SR Ca^{2+} release results). Ikemoto et al. (1989) showed that the luminal Ca^{2+} effect on the SRRC only occurs when CSQ is present, implying that the binding of Ca^{2+} to CSQ may indeed be the source of feedback to the SRRC.

An important concept can be inferred from the sigmoidal responses described above: a threshold SR Ca^{2+} load is necessary to elicit a CSQ or SRRC reaction or a CICR response (e.g., Bassani et al. (1995) observed only 3.6% SR fractional Ca^{2+} release when the SR Ca^{2+} content was 54.7 μmol/L cell H_2O). In support of this concept, Gilchrist et al. (1992) demonstrated that SR vesicles would not release Ca^{2+} when below a threshold level of luminal [Ca^{2+}]. One possible explanation is that the SRRC-CSQ control loop produces an inhibitory feedback when the SR Ca^{2+} load is sufficiently reduced.

The interface for feedback between the SRRC and CSQ remains open for speculation at present. One possible link lies in the physical connection between the SRRC and CSQ, which are anchored together with junctin and triadin, forming a stable complex (Zhang et al., 1997). In the presence of this physical connection, Ca^{2+}-binding-induced conformational changes of CSQ and SRRC have the potential to manifest changes in the entire SRRC-CSQ complex.

With regard to the above evidence for a bidirectional feedback mechanism, we speculate that 1) the binding of Ca^{2+} to the SRRC fast site induces the SRRC to undergo a conformational change to the open state, 2) which in turn affects the SRRC-CSQ complex such that the CSQ-Ca^{2+} binding curve shifts, 3) resulting in an apparent change in the CSQ dissociation constant, and then ultimately a release of Ca^{2+} from the CSQ. 4) As Ca^{2+} dissociates from the CSQ, the CSQ undergoes a conformational change, 5) which affects the SRRC-CSQ complex such that the dissociation constant of the SRRC slow closing site is altered, 6) which would affect the SRRC probability of opening (and the rate constant of Ca^{2+} release).

In this model, the bidirectional interplay was represented as feedback-induced shifts in the Ca^{2+} binding curves of CSQ and SRRCs. These curve shifts were represented in a simplified form as adjustments in the Ca^{2+} dissociation constants of CSQ and the SRRCs. With this simplification, an adjustment was not implemented with incremental changes over a range of feedback, but instead as a step change at a midrange value for the feedback. For instance, SR luminal Ca^{2+} feedback to the SRRC was represented in specific SR regions that were involved in a CICR response as a decrease in the dissociation constant of the SRRC slow site ($\sim 10 * k_{on2}$) when [Ca^{2+}CSQ] was below 5×10^{-4} M. Similarly, in SR regions undergoing CICR, the trigger-induced CSQ Ca^{2+} release was modeled by introducing an increase in the CSQ dissociation constant ($\sim$20-fold), when the fraction of SRRC in the open state was >0.15. In addition, to represent the whole-cell response, the thresholds and associated adjustments were subjected to composite averaging to account for SR regions with activated versus nonactivated SRRCs. The magnitude of the above-modeled affinity changes was chosen to approximate a 10-fold change in affinity that was observed with the binding of labeled ryanodine to the CSQ (Gilchrist et al., 1992).

Quiescent concentration of free Ca^{2+} in the cytosol

The quiescent concentration of free Ca^{2+} in the cytosol was set at 1.0×10^{-7} M from a range of 4.0×10^{-8} to 1.6×10^{-7} M (Bers, 1993; Frampton et al., 1991; Moore et al., 1991; Satoh et al., 1997). This value was key in the determination of the quiescent values of concentrations of free Ca^{2+} in the SR and the fuzzy space, determined by numerical methods described in Materials and Methods. This part of the model was supported by the outcome of the simulated value of the SR Ca^{2+} content, 201 μM, which was close to the expected value, 182 μM, converted from the value of Shannon and Bers (1997).

This work was supported in part by U.S. Public Health Service grants HL40306 and AG13987. Some of this work was presented in abstract form at the 1999 Annual Biophysical Society Meeting.

REFERENCES

Backx, P. H., W.-D. Gao, M. D. Asan-Backx, and E. Marban. 1995. The relationship between contractile force and intracellular [Ca^{2+}] in intact rat cardiac trabeculae. *J. Gen. Physiol.* 105:1–19.

Bassani, J. W. M., R. A. Bassani, and D. M. Bers. 1994. Relaxation in rabbit and rat cardiac cells: species-dependent differences in cellular mechanisms. *J. Physiol. (Lond.).* 476:279–293.

Bassani, W. M., and D. M. Bers. 1995. Rate of diastolic Ca^{2+} release from the sarcoplasmic reticulum of intact rabbit and rat ventricular myocytes. *Biophys. J.* 68:2015–2022.

Bassani, W. M., W. Yuan, and D. M. Bers. 1995. Fractional SR Ca release is regulated by trigger Ca and SR Ca content in cardiac myocytes. *Am. J. Physiol.* 268:C1313–C1329.

Berlin, J. R., J. W. M. Bassani, and D. M. Bers. 1994. Intrinsic cytosolic calcium buffering properties of single rat cardiac myocytes. *Biophys. J.* 67:1775–1787.

Bers, D. 1989. SR Ca loading in cardiac muscle preparations based on rapid cooling contracture. *Am. J. Physiol.* 256:C109–C120.

Bers, D. M. 1993. Excitation-Contraction Coupling and Cardiac Contractile Force. Kluwer Academic Publishers, London.

Bers, D. M., and J. R. Berlin. 1995. Kinetics of $[Ca]_i$ decline in cardiac myocytes depend on peak $[Ca]_i$. *Am. J. Physiol.* 268:C271–C277.

Bers, D. M., W. J. Lederer, and J. R. Berlin. 1990. Intracellular Ca transients in rat cardiac myocytes: role of Na-Ca exchange in excitation-contraction coupling. *Am. J. Physiol.* 258:C944–C954.

Bers, D. M., and V. M. Stiffel. 1993. Ratio of ryanodine to dihydropyridine receptors in cardiac and skeletal muscle and implications for e-c coupling. *Am. J. Physiol.* 264:C1587–C1593.

Bouchard, R., and D. Bose. 1989. Analysis of the interval-force relationship in rat and canine ventricular myocardium. *Am. J. Physiol.* 257: H2036–H2047.

Brandt, N. R., A. H. Caswell, S. Wen, and J. A. Talvenheimo. 1990. Molecular interactions of the junctional foot protein and dihydropyridine receptor in skeletal muscle triads. *J. Membr. Biol.* 113:237–251.

Cannell, M. B., J. R. Berlin, and W. J. Lederer. 1987. Effect of membrane potential changes on the calcium transient in single rat cardiac muscle cells. *Science.* 238:1419–1423.

Cannell, M. B., H. Cheng, and W. J. Lederer. 1994. Spatial non-uniformities in $[Ca^{2+}]_i$ during excitation-contraction coupling in cardiac myocytes. *Biophys. J.* 67:1942–1956.

Chen, D., L. Xu, A. Tripathy, G. Meissner, and B. Eisenberg. 1997. Permeation through the calcium release channel of cardiac muscle. *Biophys. J.* 73:1337–1354.

Cheng, H., M. R. Lederer, W. R. Lederer, and M. B. Cannell. 1996. Calcium sparks and $[Ca^{2+}]_i$ waves in cardiac myocytes. *Am. J. Physiol.* 270:C148–C159.

Coronado, R., J. Morrissette, M. Sukhareva, and D. M. Vaughn. 1994. Structure and function of ryanodine receptors. *Am. J. Physiol.* 266: C1485–C1504.

Delbridge, L. M. D., J. W. M. Bassani, and D. M. Bers. 1996. Steady-state twitch Ca^{2+} fluxes and cytosolic Ca^{2+} buffering in rabbit ventricular myocytes. *Am. J. Physiol.* 270:C192–C199.

Delbridge, L. M. D., H. Satoh, W. Yuan, J. W. M. Bassani, M. Qi, K. S. Ginsburg, A. M. Samarel, and D. M. Bers. 1997. Cardiac myocyte volume, Ca^{2+} fluxes, and sarcoplasmic reticulum loading in pressure-overload hypertrophy. *Am. J. Physiol.* 272:H2425–H2435.

Donoso, P., P. Humberto, and C. Hidalgo. 1995. Luminal calcium regulates calcium release in triads isolated from frog and rabbit skeletal muscle. *Biophys. J.* 68:507–515.

Earm, Y. E., and D. Noble. 1989. A model of the single atrial cell: relation between calcium current and calcium release. *Proc. R. Soc. Lond. B.* 240:83–96.

Fabiato, A. 1985. Time and calcium dependence of activation an inactivation of calcium-induced release of calcium from the sarcoplasmic reticulum of a skinned canine cardiac Purkinje cell. *J. Gen. Physiol.* 85:247–289.

Frampton, J. E., C. H. Orchard, and M. R. Boyett. 1991. Diastolic, systolic, and sarcoplasmic reticulum $[Ca^{2+}]$ during inotropic interventions in isolated rat myocytes. *J. Physiol. (Lond.).* 437:351–375.

Gilchrist, J. S. C., A. N. Belcastro, and S. Katz. 1992. Intraluminal Ca^{2+} dependence of Ca^{2+} and ryanodine-mediated regulation of skeletal muscle sarcoplasmic reticulum Ca^{2+} release. *J. Biol. Chem.* 267: 20850–20856.

Ginsburg, K. S., C. R. Weber, and D. M. Bers. 1998. Control of maximum sarcoplasmic reticulum Ca load in intact ferret ventricular myocytes. *J. Gen. Physiol.* 111:491–504.

Glukhovsky, A., D. Adam, G. Amitzur, and S. Sideman. 1998. Mechanism of Ca^{2+} release from the sarcoplasmic reticulum: a computer model. *Ann. Biomed. Eng.* 26:213–229.

Grynkiewicz, G., M. Poenie, and R. Y. Tsien. 1985. A new generation of Ca^{2+} indicators with greatly improved fluorescence properties. *J. Biol. Chem.* 260:3440–3450.

Gyorke, I., and S. Gyorke. 1998. Regulation of the cardiac ryanodine receptor channel by luminal Ca^{2+} involves luminal Ca^{2+} sensing sites. *Biophys. J.* 75:2801–2810.

Han, S., A. Schiefer, and G. Isenberg. 1994. Ca^{2+} load of guinea-pig ventricular myocytes determines efficacy of brief Ca^{2+} currents as trigger for Ca^{2+} release. *J. Physiol. (Lond.).* 480:411–421.

Harrison, S. M., E. McCall, and M. R. Boyett. 1992. The relationship between contraction and intracellular sodium in rat and guinea-pig ventricular myocytes. *J. Physiol. (Lond.).* 449:517–550.

Hidalgo, C., P. Donoso, and P. H. Rodriguez. 1996. Protons induce calsequestrin conformational changes. *Biophys. J.* 71:2130–2137.

Hilgemann, D. W., A. Collins, and S. Matsuoka. 1992. Steady-state and dynamic properties of cardiac sodium-calcium exchange. *J. Gen. Physiol.* 100:933–961.

Hilgemann, D. W., and D. Noble. 1987. Excitation-contraction coupling and extracellular calcium transients in rabbit atrium: reconstruction of basic cellular mechanisms. *Proc. R. Soc. Lond. B.* 230:163–205.

Hove-Madsen, L., and D. M. Bers. 1993. Passive Ca buffering and SR Ca uptake in permeabilized rabbit ventricular myocytes. *Am. J. Physiol.* 264:C677–C668.

Ikemoto, N., B. Antoniu, J. Kang, L. G. Mesazaros, and M. Ronjat. 1991. Intravesicular calcium transient during calcium release from sarcoplasmic reticulum. *Biochemistry.* 30:5230–5237.

Ikemoto, N., M. Ronjat, L. G. Meszaros, and M. Koshita. 1989. Postulated role of calsequestrin in the regulation of calcium release from sarcoplasmic reticulum. *Biochemistry.* 28:6764–6771.

Isenberg, G., and S. Han. 1994. Gradation of Ca^{2+}-induced Ca^{2+} release by voltage-clamp pulse duration in potentiated guinea-pig ventricular myocytes. *J. Physiol. (Lond.).* 480:423–438.

Jafri, M. S., J. J. Rice, and R. L. Winslow. 1998. Cardiac Ca^{2+} dynamics: the roles of ryanodine receptor adaptation and sarcoplasmic reticulum load. *Biophys. J.* 75:1149–1168.

Janczewski, A. M., H. A. Spurgeon, M. D. Stern, and E. G. Lakatta. 1995. Effects of sarcoplasmic reticulum Ca^{2+} load on the gain function of Ca^{2+} release by Ca^{2+} current in cardiac cells. *Am. J. Physiol.* 268: H916–H920.

Kawasaki, T., and M. Kasai. 1994. Regulation of calcium channel in sarcoplasmic reticulum by calsequestrin. *Biochem. Biophys. Res. Commun.* 199:1120–1127.

Kihara, Y., and J. Morgan. 1991. Abnormal Ca^{2+} handling is the primary cause of mechanical alternans: study of ferret ventricular muscles. *Am. J. Physiol.* 261:H1746–H1755.

Kim, D. H., S. T. Ohnishi, and N. Ikemoto. 1983. Kinetic studies of calcium release from sarcoplasmic reticulum in vitro. *J. Biol. Chem.* 258:9662–9668.

Konishi, F., and J. R. Berlin. 1993. Ca transients in cardiac myocytes measured with a low affinity fluorescent indicator, furaptra. *Biophys. J.* 64:1331–1343.

Langer, G. A., and A. Peskoff. 1996. Calcium concentration and movement in the diadic cleft space of the cardiac ventricular cell. *Biophys. J.* 70:1169–1182.

Lederer, W., E. Niggli, and R. Hadley. 1990. Sodium-calcium exchange in excitable cells: fuzzy space. *Science.* 248:283.

Legato, M. J. 1979. Cellular mechanisms of normal growth in the mammalian heart. II. A quantitative and qualitative comparison between right and left ventricular myocytes in the dog from birth to five months of age. *Circ. Res.* 44:263–279.

Li, L., G. Chu, E. G. Kranias, and D. M. Bers. 1998. Cardiac myocyte calcium transport in phospholamban knockout mouse: relaxation and endogenous CaMKII effects. *Am. J. Physiol.* 274:H1335–H1347.

Lukyanenko, V., I. Gyorke, and S. Gyorke. 1996. Regulation of calcium release by calcium inside the sarcoplasmic reticulum in ventricular myocytes. *Pflugers Arch.* 432:1047–1054.

Lukyanenko, V., A. Smirnov, and S. Gyorke. 2000. Dynamic regulation of SR Ca content by lumenal Ca-sensitive leak through RYRs in rat cardiomyocytes. *Biophys. J.* 78:440A (Abstr.).

Marcus, Y. 1997. Ion transport. *In* Ion Properties. Marcel Dekker, New York. 159–176.

Mattiazzi, A., L. Hove-Madsen, and D. M. Bers. 1994. Protein kinase inhibitors reduce SR Ca transport in permeabilized cardiac myocytes. *Am. J. Physiol.* 267:H812–H820.

McCall, E., K. S. Ginsburg, R. A. Bassani, T. R. Shannon, M. Qi, A. M. Samarel, and D. M. Bers. 1998. Ca flux, contractility, and excitation-contraction coupling in hypertrophic rat ventricular myocytes. *Am. J. Physiol.* 274:H1348–H1360.

Mokelke, E. A., B. M. Palmer, J. Y. Cheung, and R. L. Moore. 1997. Endurance training does not affect intrinsic calcium current characteristics in rat myocardium. *Am. J. Physiol.* 273:H1193–H1197.

Moore, R. L., T. I. Musch, R. V. Yelamurty, J. R. C. Scaduto, A. M. Semanchick, M. Elensky, and J. Y. Cheung. 1993. Chronic exercise alters contractility and morphology of isolated rat cardiac myocytes. *Am. J. Physiol.* 264:C1180–C1189.

Moore, R. L., and J. T. Stull. 1984. Myosin light chain phosphorylation in fast and slow skeletal muscle in situ. *Am. J. Physiol.* 247:C462–C471.

Moore, R. L., R. V. Yelamarty, H. Misawa, J. R. C. Scaduto, D. G. Pawlush, M. Elensky, and J. Y. Cheung. 1991. Altered Ca^{2+} dynamics in single cardiac myocytes from renovascular hypertensive rats. *Am. J. Physiol.* 260:C327–C337.

Ohkura, M., T. Ide, K. Furukawa, T. Kawasaki, M. Kasai, and Y. Ohizumi. 1995. Calsequestrin is essential for the Ca^{2+} release induced by myotoxin $\propto$ in skeletal muscle sarcoplasmic reticulum. *Can. J. Physiol. Pharmacol.* 73:1181–1185.

O'Neill, S., C. Overend, W. Adams, and D. Eisner. 1999. Calcium content of rat ventricular sarcoplasmic reticulum is limited by leak not uptake. *Biophys. J.* 76:A308 (Abstr.).

Page, E. 1978. Quantitative ultrastructural analysis in cardiac membrane physiology. *Am. J. Physiol.* 235:C147–C158.

Page, E., L. P. McCallister, and B. Power. 1971. Stereological measurements of cardiac ultrastructures implicated in excitation-contraction coupling. *Proc. Natl. Acad. Sci. USA.* 68:1465–1466.

Palmer, B. M., J. M. Lynch, S. M. Snyder, and R. L. Moore. 1999a. Effects of chronic run training on sodium-dependent calcium efflux from rat left ventricular myocytes. *J. Appl. Physiol.* 86:584–591.

Palmer, B. M., M. C. Olsson, J. M. Lynch, L. C. Mace, S. M. Snyder, S. Valent, and R. L. Moore. 1999b. Chronic run training suppresses alpha-adrenergic response of rat cardiocytes and isovolumic left ventricle. *Am. J. Physiol.* 277:H2136–H2144.

Peskoff, A., J. A. Post, and G. A. Langer. 1992. Sarcolemmal calcium binding sites in heart. II. Mathematical model for diffusion of calcium released from the sarcoplasmic reticulum into the diadic region. *J. Membr. Biol.* 129:59–69.

Philipson, K. D., and A. Y. Nishimoto. 1981. Efflux of Ca^{2+} from cardiac sarcolemmal vesicles. *J. Biol. Chem.* 256:3698–3702.

Radermacher, M., V. Rao, R. Grassucci, J. Frank, A. P. Timerman, S. Fleischer, and T. Wagenknecht. 1994. Cryo-electron microscopy and three-dimensional reconstruction of the calcium release channel/ryanodine receptor from skeletal muscle. *J. Cell Biol.* 127:411–423.

Reeves, J. P., and J. L. Sutko. 1983. Competitive interactions of sodium and calcium with the sodium-calcium exchange system of cardiac sarcolemmal vesicles. *J. Biol. Chem.* 258:3178–3182.

Rice, J. J., M. S. Jafri, and R. L. Winslow. 1999. Modeling gain and gradedness of Ca^{2+} release in the functional unit of the cardiac diadic space. *Biophys. J.* 77:1871–1884.

Santana, L. F., H. Cheng, A. M. Gomez, M. B. Cannell, and W. J. Lederer. 1996. Relation between the sarcolemmal Ca^{2+} current and Ca^{2+} sparks and local control theories for cardiac excitation-contraction coupling. *Circ. Res.* 78:166–171.

Satoh, H., L. A. Blatter, and D. M. Bers. 1997. Effects of $[Ca^{2+}]_i$, SR Ca^{2+} load, and rest on Ca^{2+} spark frequency in ventricular myocytes. *Am. J. Physiol.* 272:H657–H668.

Satoh, H., H. Katoh, P. Velez, M. Fill, and D. M. Bers. 1998. Bay K 8644 increases resting Ca^{2+} spark frequency in ferret ventricular myocytes independent of Ca influx. *Circ. Res.* 83:1192–1204.

Sham, J. S. K., L. Cleeman, and M. Morad. 1995. Functional coupling of Ca^{2+} channels and ryanodine receptors in cardiac myocytes. *Proc. Natl. Acad. Sci. USA.* 92:121–125.

Sham, J., L. Song, Y. Chen, L. Deng, M. Stern, E. Lakatta, and H. Cheng. 1998. Termination of Ca^{2+} release by a local inactivation of ryanodine receptors in cardiac myocytes. *Proc. Natl. Acad. Sci. USA.* 95: 15096–15101.

Shannon, T. R., and D. M. Bers. 1997. Assessment of intra-SR free [Ca] and buffering in rat heart. *Biophys. J.* 73:1524–1531.

Shannon, T. R., K. S. Ginsburg, and D. M. Bers. 2000. Reverse mode of the sarcoplasmic reticulum calcium pump and load-dependent cytosolic calcium decline in voltage-clamped cardiac ventricular myocytes. *Biophys. J.* 78:322–333.

Sipido, K. R., and W. G. Wier. 1991. Flux of Ca^{2+} across the sarcoplasmic reticulum of guinea-pig cardiac cells during excitation-contraction coupling. *J. Physiol. (Lond.).* 435:605–630.

Sitsapesan, R., and A. J. Williams. 1997. Regulation of current flow through ryanodine receptors by luminal Ca^{2+}. *J. Membr. Biol.* 159:179–185.

Smith, G. D., J. E. Keizer, M. D. Stern, J. Lederer, and H. Cheng. 1998. A simple numerical model of calcium spark formation and detection in cardiac myocytes. *Biophys. J.* 75:15–32.

Spencer, C. I., and J. R. Berlin. 1995. Control of sarcoplasmic reticulum calcium release during calcium loading in isolated rat ventricular myocytes. *J. Physiol. (Lond.).* 488:267–279.

Stauffer, B. L., B. M. Palmer, A. Hazel, J. Y. Cheung, and R. L. Moore. 1997. Hypertension alters rapid cooling contractures in single rat cardiocytes. *Am. J. Physiol.* 272:C1000–C1006.

Stern, M. D. 1992. Theory of excitation-contraction coupling in cardiac muscle. *Biophys. J.* 63:497–517.

Stienen, G. J. M., R. Zaremba, and G. Elzinga. 1995. ATP utilization for calcium uptake and force production in skinned muscle fibres of *Xenopus laevis*. *J. Physiol. (Lond.).* 482:109–122.

Szmacinski, H., and J. Lakowicz. 1995. Possibility of simultaneously measuring low and high calcium concentrations using fura-2 lifetime-based sensing. *Cell Calcium.* 18:64–75.

Tang, Y., and H. G. Othmer. 1994. A model of calcium dynamics in cardiac myocytes based on the kinetics of ryanodine-sensitive calcium channels. *Biophys. J.* 67:2223–2235.

Tibbits, G. F., H. Kashihara, and K. O'Reilly. 1989. Na^+-Ca^{2+} exchange in cardiac sarcolemma: modulation of Ca^{2+} affinity by exercise. *Am. J. Physiol.* 256:C638–C643.

Tillotson, D., and E. Nasi. 1985. The rate of diffusion of Ca^{2+} and Ba^{2+} in a nerve cell body. *Biophys. J.* 47:735–738.

VanHardeveld, C., V. J. A. Shouten, A. Muller, E. T. V. D. Meulen, and G. Elzinga. 1995. Exposure of energy-depleted rat trabeculae to low pH improves contractile recovery: role of calcium. *Am. J. Physiol.* 268: H1510–H1520.

Wibo, M., G. Bravo, and T. Godfraind. 1991. Postnatal maturation of excitation-contraction coupling in rat ventricle in relation to the subcellular localization and surface density of 1,4-dihydropyridine and ryanodine receptors. *Circ. Res.* 68:662–673.

Wier, W. G., T. M. Egan, J. R. Lopez-Lopez, and C. W. Balke. 1994. Local control of excitation-contraction coupling in rat heart cells. *J. Physiol. (Lond.).* 474:463–471.

Wohlfart, B. 1982. Analysis of mechanical alternans in rabbit papillary muscle. *Acta. Physiol. Scand.* 115:405–414.

Wong, A., A. Fabiato, and J. Bassingthwaigthe. 1992. Model of calcium-induced calcium release mechanism in cardiac cells. *Bull. Math. Biol.* 54:95–116.

Yuan, W., K. S. Ginsburg, and D. M. Bers. 1996. Comparison of sarcolemmal calcium channel current in rabbit and rat ventricular myocytes. *J. Physiol. (Lond.).* 493:733–746.

Zhang, L., J. Kelley, G. Schmeisser, Y. M. Kobayashi, and L. R. Jones. 1997. Complex formation between junctin, triadin, calsequestrin, and the ryanodine receptor. *J. Biol. Chem.* 272:23389–23397.